Treponema pallidum subsp. *pallidum* with an Artificially Impaired TprK Antigenic Variation System is Attenuated in the Rabbit Model of Syphilis

Emily Romeis[1], Nicole A. P. Lieberman[2], Barbara Molini[1], Lauren C. Tantalo[1], Benjamin Chung[2], Quynh Phung[2], Carlos Avendaño[2], Anastassia Vorobieva[3,4], Alexander L. Greninger[2,5] and Lorenzo Giacani[1,6*]

[1]Department of Medicine, Division of Allergy and Infectious Diseases, University of Washington, Seattle, WA, USA

[2]Department of Laboratory Medicine and Pathology, University of Washington, Seattle, WA, USA

[3]VIB-VUB Center for Structural Biology, VIB, Brussels, Belgium

[4]Structural Biology Brussels, Vrije Universiteit Brussel, Brussels, Belgium

[5]Vaccine and Infectious Disease Division, Fred Hutchinson Cancer Research Center, Seattle, WA, USA

[6]Department of Global Health, University of Washington, Seattle, WA, USA

[*]Corresponding Author: giacal@u.washington.edu

Short title: Impairing the *T. pallidum* TprK system

Abstract

Background. The TprK protein of the syphilis agent, *Treponema pallidum* subsp. *pallidum* (*T. pallidum*), undergoes antigenic variation in seven discrete variable (V) regions via non-reciprocal segmental gene conversion. These recombination events transfer information from a repertoire of 53 silent chromosomal donor cassettes (DCs) into the single *tprK* expression site to continually generate TprK variants. Several lines of research developed over the last two decades support the theory that this mechanism is central to *T. pallidum*'s ability for immune avoidance and persistence in the host. Structural and modeling data, for example, identify TprK as an integral outer membrane porin with the V regions exposed on the pathogen's surface. Furthermore, infection-induced antibodies preferentially target the V regions rather than the predicted β-barrel scaffolding, and sequence variation abrogates the binding of antibodies elicited by antigenically different V regions. Here, we engineered a *T. pallidum* strain to impair its ability to vary TprK and assessed its virulence in the rabbit model of syphilis.

Principal findings. A suicide vector was transformed into the wild-type (WT) SS14 *T. pallidum* isolate to eliminate 96% of its *tprK* DCs. The resulting SS14-DC^{KO} strain exhibited an *in vitro* growth rate identical to the untransformed strain, supporting that the elimination of the DCs did not affect strain viability in absence of immune pressure. In rabbits injected intradermally with the SS14-DC^{KO} strain, generation of new TprK sequences was impaired, and the animals developed attenuated lesions with a significantly reduced treponemal burden compared to control animals. During infection, clearance of V region variants originally in the inoculum mirrored the generation of antibodies to these variants, although no new variants were generated in the SS14-DC^{KO} strain to overcome immune pressure. Naïve rabbits that received lymph node extracts from animals infected with the SS14-DC^{KO} strain remained uninfected.

Conclusion. These data further support the critical role of TprK in *T. pallidum* virulence and persistence during infection.

Author Summary

Syphilis is still endemic in low- and middle-income countries, and it has been resurgent in high-income nations, including the U.S., for years. In endemic areas, there is still significant morbidity and mortality associated with this disease, particularly when its causative agent, the spirochete *Treponema pallidum* subsp. *pallidum* (*T. pallidum*) infects the fetus during pregnancy. Improving our understanding of syphilis pathogenesis and *T. pallidum* biology could help investigators devise better control strategies for this serious infection. Now that tools to genetically manipulate this pathogen are available, we can engineer *T. pallidum* strains lacking specific genes or genomic regions known (or believed) to be associated with virulence. This approach can shed light on the role of the ablated genes or sequences in disease development using loss-of-function strains. Here, we derived a knockout (KO) *T. pallidum* mutant (SS14-DC^{KO}) impaired in its ability to undergo antigenic variation of TprK, a protein that has long been hypothesized to be central in evasion of the host immune response and pathogen persistence during infection. When compared to the WT isolate, which is still capable of antigenic variation, the SS14-DC^{KO} strain is significantly attenuated in its ability to proliferate and to induce early disease manifestations in infected rabbits. Our results further support the importance of TprK antigenic variation in syphilis pathogenesis and pathogen persistence.

Introduction

Syphilis is a chronic sexually transmitted infection that still represents a concern for public health as it causes significant morbidity and mortality worldwide. The World Health

Organization (WHO) estimated that syphilis global incidence is between 5.6 to 11 million new cases every year, while global prevalence ranges between 18 to 36 million cases (1, 2). Although most cases occur in low- and middle-income countries where the disease is endemic, syphilis rates have been on the rise for years in high-income nations, primarily among men who have sex with men (MSM), even though the gap in incidence between MSM and the heterosexual population is gradually reducing (3-8). In the US, the rate of early syphilis in 2020 (12.7 cases per 100,000 population) represented a 504% increase compared to the rate reported in 2000 (2.1 cases per 100,000 population) (3). Furthermore, about 1.4 million pregnant women a year acquire syphilis worldwide. Congenital syphilis (CS), resulting from the ability of *Treponema pallidum* subsp. *pallidum* (*T. pallidum*) to colonize and cross the placenta, causes an estimated 305,000 annual cases of fetal loss or stillbirth and 215,000 infants born prematurely and/or with clinical signs of infection (9-11).

In untreated subjects, primary and secondary syphilis generally manifests in distinct clinical stages, followed by a period of asymptomatic latency that, in most cases, will last for the patient's lifetime (12). Data preceding the introduction of penicillin for syphilis treatment showed that in about 30% of patients, the disease would reactivate after years to decades from the onset of latency and progress to its tertiary stage and its most serious manifestations (13). Key to this decades-long persistence is the pathogen's ability to evade the robust host immune response that develops during infection. This central feature of *T. pallidum* virulence has long been attributed to antigenic variation of the TprK (Tp0897) protein (12). This putative integral outer-membrane porin (14) harbors seven discrete variable regions (V1-V7), each predicted by AlphaFold2 (https://AlphaFold.ebi.ac.uk/) to form an external loop at the host-pathogen interface (Fig.1). Sequence variability within the V regions is generated through non-reciprocal segmental

gene conversion, a process that transfers information contained in 53 silent chromosomal donor cassettes (DCs) into the *tprK* expression site (15, 16), located ~175 kbp away from the DCs. Most of the DCs (51/53; 96%) are located downstream of the *tprD* gene (*tp0131*) at nucleotide (nt) position 148,435-152,400, while the remaining two DCs are downstream of the *tp0136* gene at position 159,499-159,576, based on the SS14 strain reference genome sequence (NC_021508.1/CP004011.1) (17). In a previous study by Addetia *et al.* (17) it was estimated that the total *tprK* diversity that could be generated by the combined usage of all DCs would range between 10^{13} - 10^{15} full-length individual TprK sequences (17).

Aside from sequence variability and potential for generation of quintillions of unique sequences, the role of TprK in immune evasion and pathogen persistence is supported by the evidence that a) sequence diversity accumulates over time during experimental infection (18), b) infection-induced antibodies preferentially target the TprK V regions rather than the predicted β-barrel scaffolding of the protein (19), c) sequence variation abrogates binding of antibodies raised to antigenically different V regions (20), d) TprK variants accumulate more rapidly in immunocompetent hosts compared to immunosuppressed rabbits as the result of immune selection (21, 22) and, lastly, e) TprK sequences found in disseminated secondary lesions in the rabbit model differ from those in the original inoculum, supporting that secondary lesions contain treponemes that avoided the initial round of immune clearance associated with the resolution of the primary lesion(s) (23).

Recently, Romeis *et al*. (24) described a procedure that successfully allowed the replacement of a specific *T. pallidum* chromosomal region with a kanamycin resistance (kan^R) cassette. This approach uses a suicide vector with the kan^R cloned between homology arms matching the regions upstream and downstream of the sequence to be deleted. This work

provided the first experimental evidence that *T. pallidum* could be genetically altered and opened the gateway for systematic derivation of KO mutants to assess their fitness and virulence *in vivo* and shed light on the role of specific genes and or genomic regions in syphilis pathogenesis. Although a *tprK*^{KO} strain could not be derived, to further explore the role of TprK in *T. pallidum* persistence, we ablated the 51 DCs situated downstream of the *tprD* gene in the SS14 *T. pallidum* strain, which resulted in an impaired TprK antigenic variation system. We then evaluated disease progression and the pathogen's ability to proliferate in rabbits infected with the mutant strain (renamed SS14-DC^{KO}) in comparison to animals infected with the WT strain, still fully capable of varying TprK.

Results

SS14-DC^{KO} mutant treponemes are not impaired in their ability to grow *in vitro* and *in vivo* in a partially immune-privileged site.

Treponemes transformed with the p*DC*arms-47p-*kan*^{R} suicide vector, designed to eliminate the DCs downstream of *tprD* through a double cross-over recombination event, were selected by propagation in selective media (Fig.2A). As a control, the parent SS14 strain was also propagated in both normal and selective media in parallel to the transformed strain. Due to the ~44 hours generation time of the SS14 strain, *T. pallidum* cells needed to be sub-cultured every 14 days until week 13 post-transformation (Passage #8; Fig.2A), and weekly thereafter. Transformed SS14-DC^{KO} treponemes had significantly recovered by 4 weeks post-transformation (Fig.2A) at the time passage #3 was harvested, and approximately 10 treponemal cells per microscopic field (corresponding to ~10^7 *T. pallidum* cells/ml) could be counted at this time. The cell density of transformed treponemes increased by week 10 and remained steady

with harvests of ~10^8 *T. pallidum* cells/ml (Fig.2A). Wild-type parent SS14 cells propagated in selective media could not be seen by dark-field microscopy (DFM) at any time and sub-culturing was stopped at week 8 (Fig.2A). Propagation of the WT parent strain was halted at week 18 (Fig.2A). DNA extracted from treponemes harvested at passage #8 post-transformation was used for qualitative amplifications (primers in Table 1) designed to confirm integration of the *tp0574* promoter-*kan*^{R} sequence where the DC-containing region used to be, as well as lack of residual transformation vector or DNA from the parent strain. Results (Fig.2B) showed that no amplification occurred in treponemal cultures with primers specific for the suicide vector backbone (subpanel #1), confirming lack of residual plasmid DNA. As expected, amplification of the *tp0574* gene was positive for both the parent SS14 and the SS14-DC^{KO} strain templates (subpanel #2), confirming the presence of treponemal DNA in both cultures. Furthermore, amplification of the target region with the reverse primer annealing downstream of the right homology arm (hence not cloned into the suicide vector) and a forward primer annealing to the *kan*^{R} gene, respectively (subpanel #3), yielded positive amplification only with template from the SS14-DC^{KO} strain, confirming that integration of the *tp0574* promoter-*kan*^{R} sequence occurred where expected. Amplification with both primers outside of the homology arms yielded amplicons of different sizes (subpanel #4; 2,982 bp for SS14-DC^{KO} and 5,980 bp for the parent strain), confirming deletion of the DCs and lack of parent SS14 DNA in the mutant strain culture. Lastly, amplification with primers specific for the *kan*^{R} only amplified the SS14-DC^{KO} and the vector control template (subpanel #5).

Rabbit intratesticular (IT) inoculation with either the WT or the SS14-DC^{KO} strain was also used to assess whether the mutant strain would be impaired in its ability to grow *in vivo* and induce orchitis. The time to orchitis in WT- and SS14-DC^{KO}-infected animals was identical (21

days post-inoculation) and, when harvested, both rabbits yielded comparable treponemal concentrations (~10^8/ml). For both animals, testes were minced and extracted in 10 ml of sterile saline.

Altogether, these data confirmed that a) the *kan*^{R} gene was integrated into the SS14-DC^{KO} strain genome in place of the targeted 51 DCs, that b) no residual suicide plasmid DNA or parent treponemes contaminated the SS14-DC^{KO} culture, that c) 96% of the DCs are missing in the mutant strain and lastly, that d) despite this deletion, SS14-DC^{KO} treponemes are not impaired in their ability to grow *in vitro* and *in vivo* compared to the WT strain.

Table 1. Primers used in this study.

Targets; application	**Forward (F) and reverse (R) primer sequences (5'-3'), and probe (P) if applicable**	**Amplicon length (bp)**	**Sub-panel # in Fig.2B**
pUC57 vector primers; sequencing, assessing plasmid carry-over	(F) TAAAACGACGGCCAGTGAAT (R) GACCATGATTACGCCAAGC	2,967	1
tp0574; qualitative PCR	(F) TGTGGCTCGTCTCATCATGA (R) CTGGGCCACTACCTTCGCAC	313	2
kan^R (F primer), right *DC* flanking region (R primer); qualitative PCR and sequencing (F)	(F) GAGCCATATTCAACGGGAGA (R) CTTCTCCTTCGCCCTCGAC	1,799	3
Left *DC* flanking region (F primer), Right *DC* flanking region (R primer); qualitative PCR	(F) CACAGAAGGGCAGCAGTACA (R) CTTCTCCTTCGCCCTCGAC	2,982 (SS14-DC^{KO}) or 5,980 (WT)	4
kan^R*;* qualitative PCR; RT-qPCR	(F) GAGCCATATTCAACGGGAGA (R) ATTCCGACTCGTCCAACATC	663	5
Left *DC* flanking region (F primer), *kan*^{R} (R primer); qualitative PCR and sequencing	(F) CACAGAAGGGCAGCAGTACA (R) ATTCCGACTCGTCCAACATC	1,846	
tp0131 (tprD); RT-qPCR	(F) CACTAGTCTTGGGGACACGC (R) TCCTGGTTGCAATTCACGTA	273	
tp0897 (tprK); RT-qPCR	(F) GAAAATCGCCTGTGCCCTAC (R) GGTTCCCCACGTTTAGTTAG	80	
tp0574; qPCR, RT-qPCR	(F) CAAGTACGAGGGGAACATCG (R) TGATCGCTGACAAGCTTAGG (P) 6FAM-CGGAGACTCTGATGGATGCTGCAGTT-NFQMGB[1]	132	
tp0127; ddPCR	(F) GCGTGTATGGAGAAGCATTG (R) CGCCTGATAGCCTATATCCAC (P) HEX-AGATATGGT/ZEN/ACTACGCGCCGC-3IABkFQ[2]	139	

kan^{R}; ddPCR	(F) CACTCAGGCGCAATCAC (R) CCAGACTTGTTCAACAGGC (P) FAM-ACGGTTTGGTTGATGCGAGTGATTT-BkFQ[3]	91
tp0001 (*dnaA*); ddPCR,	(F) CTCATGGAAATACTGCTCC (R) CGGATACAAAGTTCTCGAAG (P) FAM-AGCTTTCACCCCGACCTGAAC-BkFQ[3]	135
tp0574 promoter; sequencing	(F) AGCGGATCCTCCCAAAAAGA (R) GATTACACCTCCGTATAGAG	N/A
pUC57 vector primers; sequencing, assessing plasmid carry-over	(F) TAAAACGACGGCCAGTGAAT (R) GACCATGATTACGCCAAGC	2,967

[1]Minor groove binder nonfluorescent quencher
[2]3′ Iowa Black fluorescence quencher
[3]Black hole fluorescence quencher

Genome sequencing and droplet digital PCR confirm deletion of 96% of the DCs, absence of additional mutations between the WT and SS14-DC^{KO} strains, and similar *tprK* expression level in WT and mutant treponemes.

At passage #2-5 (Week 2-6 post-transformation in Fig.2A), ahead of genome sequencing, DNA extracted from SS14-DC^{KO} and parent SS14 cells was processed for quantitative droplet digital PCR (ddPCR) to calculate copy number of the *kan*^{R} and *tp0127* (contained within the eliminated region containing the DCs) genes, normalized to the copy number of *dnaA* gene (*tp0001*; present in both parent and transformed treponemes). The normalized ratios of either *kan*^{R} or *tp0127* were expected to be either zero or ~1.0 depending on the strain analyzed. When the parent SS14 DNA was used as control, the *tp0127*:*dnaA* was near 1.0 over the four analyzed passages (Fig.3A), while the *kan*^{R}:*dnaA* ratio was zero due to lack of the *kan*^{R} gene in this strain (Fig.3A). In the SS14-DC^{KO} strain, the *kan*^{R}:*dnaA* ratio neared 1.0 when DNA from passage #3 and #4 was analyzed (Fig.3A), and was 1.0 for passage #5, while the *tp0127*:*dnaA* ratio was zero (due to the absence of *tp0127*), with the exception of passage #2. This result was however expected due to the presence of residual parent SS14 DNA, given that the culture had not been

passaged yet after transformation (Fig.3A). These data reiterated that a) integration of the *kan*^{R} gene occurred in the DC locus and supported that no extra copies of the *kan*^{R} gene existed outside or within the SS14-DC^{KO} strain genome. As previously discussed (24), the slightly <1.0 results in some of these assays are likely due to the proximity of the *dnaA* gene (nt position 4-1,395 in the SS14 genome) to the chromosomal origin of replication.

To ascertain that DC deletion did not affect *tprK* transcription, cDNA generated from the SS14-DC^{KO} and WT strain RNA, was used to assess transcription of the *tprK* (*tp0897*) and *tp0574* genes (used as housekeeping gene; primers in Table 1). Message quantification (Fig.3B) showed that, like in other *T. pallidum* strains (25), *tprK* is poorly expressed in the SS14 strain compared to *tp0574*, but its expression does not differ significantly between the WT and mutant strains.

Whole genome sequencing (WGS) performed on SS14-DC^{KO} treponemes from passage #9 confirmed the absence of reads for the *tprK* DCs in the SS14-DC^{KO} strain following assembly to the SS14 reference genome (Fig.3C). Assembly using a reference genome where the DCs were replaced *in silico* with the *kan*^{R} cassette (KO reference) was consistent with the replacement of the 51 DCs downstream of *tprD* with the *tp0574* promoter-*kan*^{R} sequence (Fig.3D). Because sequencing used enrichment probes specific for multiple WT *T. pallidum* genomes, coverage of the *kan*^{R} gene (Fig.3D) was slightly lower than the average compared to the rest of *T. pallidum* genome. A search for reads matching the suicide vector backbone yielded no results, confirming lack of residual suicide vector DNA. These results further confirmed elimination of 96% of the DCs (schematically represented in Fig.3E) in the SS14-DC^{KO} strain and their replacement with the *kan*^{R} cassette. Furthermore, these data showed that despite this deletion, mutant treponemes are not impaired in their ability to express *tprK* compared to the WT

strain. The WT parent strain propagated in parallel to the mutant strain was also sequenced as a control. As expected, in the WT strain the DC locus is intact (Fig.3F), while a gap is visible where the *kan*^{R} cassette is located when reads from the WT strain were assembled to the KO reference (Fig. 3G). A thorough comparison of the WT and KO genomes to evaluate the presence of additional "background" mutations that could have arisen in the KO strain showed no differences between the WT and KO strains outside of the DC locus.

To assess whether the replacement of the DCs induced transcriptional modifications of downstream genes that, in turn, could affect the outcome of the *in vivo* experiments, we quantified the mRNA of the *tp0131* gene in both the WT and mutant strains. In the WT, the *tp0131* gene immediately follows the DCs, and both this gene and the DCs are in the reverse orientation relative to the genome (Fig.3E). In the mutant strain, *tp0131* remains immediately downstream of the inserted transgene, but in reverse orientation, while the *kan*^{R} cassette is in forward orientation (Fig.3E). All quantifications were normalized to the mRNA of the *tp0574* gene. Quantification of the *kan*^{R} mRNA was also performed as a control, as the *tp0574* minimal promoter also drives transcription of the resistance cassette in the mutant strain, but no *kan*^{R} gene is present in the WT. Results (Fig.3H/I) showed that expression of *tp0131* was not significantly different in the two strains, regardless of whether the transcript was reverse transcribed using a *tp0131*-specific primer (GSP) or random hexamers (RE). These results support that *tp0131* transcription is not affected by the replacement of the DCs and that there is no transcription of the *tp0131* non-coding strand (possibly originating from the *kan*^{R} cassette-associated promoter), which reverse transcription with RE would have captured. Overall, however, because *tp0131* transcription is not significantly different in these strains, these data support the absence of polar transcriptional effects in the SS14-DC^{KO} strain due to the insertion of the resistance cassette. As

seen in our previous study (24), the *kan*^{R} message in the mutant strain was comparable, albeit slightly lower, to that of *tp0574* (Fig.3I).

Early lesion development is attenuated in rabbits infected with treponemes lacking most DCs.

Differences in early lesion development were assessed in New Zealand White rabbits infected intradermally (ID) in multiple sites on their shaved backs with either the WT or mutant strain. Following infection of two groups of four rabbits each, animals were regularly monitored to measure lesion diameter. Samples were collected every ~10 days for quantification of treponemal burden (both biopsies and aspirates) and *tprK* deep sequencing (biopsies only). Serum samples were collected weekly for syphilis serology using both a non-treponemal (Venereal Disease Research Laboratory; VDRL) and treponemal (*Treponema pallidum* particle agglutination; TPPA) test. The diameter of primary lesions in rabbits infected with the WT strain became significantly larger ($p<0.0001$) compared to the lesions induced by the SS14-DC^{KO} strain starting at day 9 post-inoculation (Fig.4A). Lesion size in SS14-DC^{KO} -infected rabbits plateaued at day 50 post-inoculation with an average diameter of 7.0 mm. In control animals, lesion size steadily increased throughout the experiment (Fig.4A) up to day 65 post-inoculation ($p>0.05$ for lesion diameter values between day 65 and day 72 in WT-infected animals) with mean diameters of 26.75 mm (day 65) and 30.3 mm (day 72), respectively. Pictures of the four animals still in the study at day 72 post-inoculation (Fig.4B) show that in addition to being significantly enlarged, all lesions in the control animals had progressed to an ulcerated state, with large central necrotic areas. In animals infected with the SS14-DC^{KO} strain, ulceration was not evident. Circled areas correspond to lesions that were not biopsied at the time the picture was taken.

In SS14-DC^{KO}-infected rabbits, treponemal burden is reduced and development of humoral immunity to infection is delayed.

Treponemal burden in lesion biopsies and needle aspirates was assessed by qPCR and DFM, respectively. In both cases (Fig.5A, B), significantly more treponemes were detected in samples from the control animals compared to those from rabbits infected with the SS14-DC^{KO} strain. Although qPCR (Fig.5A) detected *T. pallidum* in all tested samples, treponemal burden in lesions induced by the mutant strain decreased by one (day 9-37), two (day 65-79), or three orders of magnitude (day 37-58) between the control and test samples. As expected, treponemal burden decreased in lesions from control animals over time due to immune clearance (13). In contrast, the overall burden in lesions from rabbits infected with the SS14-DC^{KO} strain remained stably low (330.6 copies/reaction in average) in samples collected at day 37-79 post-inoculation. No treponemes were detected by DFM of needle aspirates collected from SS14-DC^{KO} -infected rabbits at any time point, while treponemes could be detected in lesions from WT-infected animals from day 37-72 post-inoculation (Fig.5B), suggesting that the treponemal burden in samples from test animals was always below the limit of detection of this assay unless rabbits were infected with the WT strain.

VDRL tests performed on serum samples collected over time showed that the WT-infected animals seroconverted earlier and reached higher titers in a shorter time compared to the SS14-DC^{KO} rabbits (Fig.5C). In rabbits infected with the mutant strain, only one rabbit had seroconverted by day 37 post-inoculation (1:2 titer). This titer, however, could not be reproduced at day 44 post-infection (Fig.5C). VDRL titers between the two rabbit groups remained significantly different from day 58 to the end of the experiment. TPPA titers were significantly

different between control and test rabbits only up to day 23 post-infection. Together, these data support impairment of the SS14-DC^{KO} strain's ability to proliferate in dermal lesions, leading to an overall lower treponemal burden and to a delayed development of VDRL and TPPA antibodies.

Rabbits used as recipients of lymph nodes from SS14-DC^{KO}-infected rabbits did not develop syphilis infection.

Immediately after euthanasia, popliteal lymph nodes were harvested from each of the ID-infected rabbits and transferred via IT injection into a naïve rabbit to assess *T. pallidum* presence. A total of four animals (two per group) were picked randomly and euthanized on day 44 post-infection. The remaining rabbits were euthanized on day 79 post-infection. Rabbits were monitored weekly for orchitis development and bled monthly to assess seroconversion, unless orchitis developed and was confirmed by visualization of treponemes in testicular aspirates, at which point the animal was deemed positive and euthanized. One animal that received lymph nodes from the control rabbits (Table 2) had developed orchitis (confirmed by treponemal presence in a needle aspirate) at day 33 post-inoculation, while two more in the same group developed orchitis (Also DFM-positive) at day 35 post-inoculation. The fourth rabbit in the group developed orchitis at day 74 post-inoculation (Table 2). In contrast, none of the recipients of lymph node extracts from rabbits infected with the SS14-DC^{KO} strain developed orchitis or seroconverted during the 3-month observation period, supporting absence of treponemal cells in these lymph node extracts at the time the RIT was performed.

Table 2. Rabbit infectivity test results

Infecting strain	RIT day	Donor Rabbit[1]	Time to positive orchitis/DFM[2]	Month 1 serology (day 30 post-RIT)		Month 2 serology (day 60 post-RIT)		Month 3 serology (day 90 post-RIT)	
				VDRL[3]	TPPA[4]	VDRL[3]	TPPA[4]	VDRL[3]	TPPA[4]
SS14-WT	Day 44 post-IDI	505	74 days	NR	NR	NP	NP		
		512	33 days	NP	NP				
	Day 79 post-IDI	510	35 days	R; 1:20	R; 1:1280				
		511	35 days	R; 1:4	R; 1:80				
SS14-DC^{KO}	Day 44 post-IDI	507	N/A	NR	NR	NR	NR	NR	NR
		503	N/A	NR	NR	NR	NR	NR	NR
	Day 79 post-IDI	501	N/A	NR	NR	NR	NR	NR	NR
		504	N/A	NR	NR	NR	NR	NR	NR

[1]Identification number of ID-infected donor rabbit. Naïve RIT rabbits received lymph-node from the donor rabbits.
[2]In rabbits with orchitis, treponemes were also detected in testicular needle aspirates using DFM.
[3]VDRL results (NR = Non-reactive; R = Reactive) and titers are shown. NP: Not performed
[4]TPPA results (NR = Non-reactive; R = Reactive) and titers are shown when measured. NP: Not performed.

SS14-DC^{KO} treponemes do not generate new TprK V region variants.

Deep sequencing was performed to define TprK isogenicity and antigenic identity in the *T. pallidum* inocula (for both the WT and SS14-DC^{KO} strains) used for rabbit ID infection and to monitor evolution of diversity over time in progressing early lesions. Table 3 shows the most abundant (>5% of the total for either strain) amino acid sequences for each V region for the WT and SS14-DC^{KO} strains, while all the detected inoculum variants are reported in Table S1.

Table 3. TprK variability profile in the SS14 and SS14-DC^{KO} strains used for rabbit ID inoculation.

V Region	Amino acid sequence	WT SS14 strain Percent sequence	SS14-DC^{KO} strain Percent sequence
V1	GIASETGGAGALKH	96.06195	81.30797
V1	GIASEKNGGAQPLKH	Not detected	14.59834
V2	WEGKDSKGVVQAGANHSK	85.1821	40.83901
V2	WEGKSNTGAPAAGANHSK	7.328483	Not detected
V2	WEGKDSQGKAPAGANHSK	1.914901	25.66107
V2	WEGKSNTGVVQAGANHSK	1.042542	29.81366
V3	TLSGDYATARAGADDILWD	88.95463	65.03622
V3	TLSGGYATARAGADDILWD	5.402198	0.476627
V3	TLSGDYAQAAGAGADDILWD	Not detected	28.20839
V4	TDVGRKKDGAQGTV	96.91317	96.16694
V5	QASNVFQGVFLTDTTPMLQHDC	53.176	1.716312
V5	QASNVFQGVFLTTPMQKDDC[1]	26.09685	0.443286
V5	QASNVFQGVFLTTPMLQHDC[1]	12.33243	68.85708
V5	KASNVFKDVFLTNAMDMQTHDC	1.511896	12.80529
V5	KASNVFKDVFLTDTTPMQTHDC[1]	Not detected	10.32818
V6	PVHWKALAPAQPPARVDIY	49.2956	Not detected
V6	PVHWKALARAQPPARVDIY[1]	27.46295	Not detected
V6	PVHWKALARARPPVPAIY[1]	Not detected	75.82605
V7	YGGTNKKNDAAPAAPATKWKAEYCGYY	56.19608	41.41053
V7	YGGTNKKNDAAPATKWKAEYCGYY	38.03072	3.803587
V7	YGGTNKQAATKWKAEYCGYY	Not detected	46.71209

[1]Synthesized as peptides for ELISA.

Results showed that neither inoculum was isogenic for *tprK*. Among all V regions, however, V4 exhibited the highest degree of antigenic identity with a single variant representing 96.9% and 96.1% of all detected sequences in the SS14 and the SS14-DC^{KO} strains, respectively (Table 3 and Table S1), while one V1 variant accounted for 96.0% and 81.3% of all sequences found in the WT and mutant strain, respectively. Both strains shared at least one highly represented (>40%) V region sequence in V2, V3, and V7. Higher heterogeneity was found in V5 and V6 (Table 3 and Table S1) compared to all the other V sequences.

TprK profiling in lesion samples collected sequentially showed that generation of new variants was impaired in SS14-DC^{KO} treponemes compared to WT treponemes for all V regions. Heatmaps showing amino acid sequence variants detected at greater than 0.25% prevalence in inoculum and biopsies are reported in Fig.6 for V6, and in Fig.S1-S6 forV1-V5, and V7, respectively. For each V region, a link to an interactive version of the graph is reported in the relative figure legend. . In V1, for example (Fig.S1), five non-inoculum variants could be detected in rabbits infected with the WT strain, while no new variants were detected in animals infected with the SS14-DC^{KO} strain. In V5 and V6 (Fig.S5 and 6) a total of 35 and 172 non-inoculum variants, respectively, were detected at greater than 0.25% prevalence in rabbits infected with the WT strain over the course of the experiment, but only 5 and 1 variants were detected in samples from animals that received the mutant strain for the same V regions. All variants detected at all time points are reported in Table S2. Based on the results shown in Fig.6 and in Fig.S1-S6, eleven putative new variants were detected in rabbits infected with the SS14-DC^{KO} strain. These variants, however, were also present in the inoculum, but their prevalence was <0.25% (Table S3). Taken together, these data support that elimination of the DCs significantly affected the generation of new TprK variants in the SS14-DC^{KO}. In addition, the two DCs downstream of the *tp0136*, predicted to preferentially recombine into V7 (17), did not contribute to generation of variability in the samples we analyzed from rabbits infected with the SS14-DC^{KO}.

Development of humoral reactivity to V region variants is limited in SS14-DC^{KO}-infected rabbits.

Synthetic peptides based on V5 and V6 sequences found in the inoculum treponemes for the WT and the SS14-DC^{KO} strains (Table 3) were used to perform ELISAs with sera from infected rabbits to evaluate whether variation in V sequence abundance would correlate with the development of a humoral immune response against these sequences. Results showed that in rabbits infected with WT treponemes, selected V regions underwent an initial expansion relatively early following treponemal ID injection compared to the inoculum (Fig.7; panels A-C). Sequence abundance, however, decreased sharply over the following 2-3 weeks and remained low throughout the remaining timepoints. Antibodies specific for these V regions could be clearly detected (Figure 7, panels D-F) at day 35 post-infection and, in some instances also at day 28 post-infection, albeit only slightly above background and not for all samples. Reactivity to a recombinant portion of TprK, corresponding to about a third of the protein, and containing two conserved loops (C1 and C2; Fig.1) was used as a control to evaluate development of immunity to the TprK antigen. These results support that the decrease in V region abundance is due to immune clearance of treponemes carrying such sequences, as also shown in earlier studies (21). On the contrary, in rabbits infected with the SS14-DC^{KO} strain (Fig.7, panels G-I) the relative abundance of the analyzed V regions either remained virtually constant or tended to increase over the first 41 days post-inoculation. No deep sequencing data could be uniformly obtained from SS14-DC^{KO} samples past day 41, due to the low treponemal burden in these samples. Antibodies towards these abundant V regions were detectable in sera from the animals infected with the KO strain only at much later time points after infection and at a much lower level compared to the sera from the WT-infected rabbits. Also the reactivity to the larger recombinant TprK fragment became evident only toward the latest time points and never reached a level comparable to that of the control animals (Fig.7, panels J-L). These results are consistent with a

slow host response to the pathogen in these rabbits due to the reduced treponemal burden at the injection site following inoculation (Fig.5A/B) which, in turn, induced a host response less robust than by rabbits infected with WT treponemes (Fig.7; as well as lesion size in Fig.4A, and TPPA and VDRL results in Fig.5C/D).

Discussion

The significant impact of syphilis on public and global health warrants research efforts to improve our understanding of the molecular mechanisms behind its pathogenesis. In turn, such efforts could aid strategies for disease control and even vaccine development. The approach to derive *T. pallidum* knockouts recently developed and validated by our groups (24) provides a novel tool to study the role of the pathogen's known or putative virulence factors by comparing loss-of-function mutants with their parent WT isolates. Even though we are still far from having all the genetic tools needed to fully satisfy Koch's molecular postulates (26) for *T. pallidum*, this approach is a significant step forward from to the use of heterologous bacterial systems transformed to express *T. pallidum* genes and perform gain-of-function assays (27-29).

With the exception of an isolated study (30), all others that focused on TprK pointed at this antigen as the chief player in pathogen immune evasion and survival during natural and experimental infection (14-18, 20-23, 31-34). The TprK-encoding *tp0897* gene, therefore, was considered a prime candidate for ablation. However, despite several independent attempts performed with a pUC57-based suicide vector identical to the one used here (but with homology arms specific for the *tprK* gene) and the same transformation/selection approach, a $tprK^{KO}$ isolate could not be derived. Although we cannot exclude that these experiments were not successful due to the difficulties of recovering treponemes post-transformation, the hypothesis that *tprK*

could be an essential *T. pallidum* gene should not be dismissed. It is intriguing that, even when deep sequencing of full-length *tprK* ORFs is performed (34), amplicons containing non-functional *tprK* sequences (e.g., due to frameshifts or stop codons within the ORF) are not found despite the heavy recombination activity occurring at this site. Aside from immune evasion, therefore, TprK could also mediate a biological function needed for *T. pallidum* survival even *in vitro*, where immune pressure is absent. Preliminary structural (14) and modeling data using AlphaFold2 (Fig.1) support this antigen as a porin transporter, a function predicted for virtually all of the Tpr proteins of *T. pallidum*, even though the nature of the transported substrate(s) is yet to be determined. This study also demonstrated that the putative *tp0127* gene is non-essential in *T. pallidum*. This small 229 codon ORF encodes a hypothetical protein with unknown function, and the gene is reported as the member of a family of paralogs that includes *tp0314, tp0315, tp0346, tp0347, tp0479, tp0617-0619, tp0697, and tp0698*, a group of short, annotated genes encoding hypothetical proteins that could possibly perform the same function of *tp0127*. This work, therefore, albeit minimally, contributes to defining the essential *T. pallidum* genome. Despite the difficulty in deriving a *tprK*^{KO} mutant, however, a strain lacking the ~4kbp region containing 96% of the DCs was readily attained, and this deletion did not produce any notable changes SS14-DC^{KO} proliferation *in vitro* or following rabbit IT infection compared to the parent strain. After the weeks needed for the mutant treponemes to recover post-transformation, the *in vitro* growth curve of the SS14-DC^{KO} strain overlapped that of its parent SS14 isolate (Fig.2A), while similar time to orchitis and identical treponemal yields were measured following rabbit infection in testes prior to the point when sufficient cellular infiltrates would induce treponemal clearance. Altogether, these data support that the SS14-DC^{KO} strain is not impaired in its ability to proliferate until a robust host immune response to the pathogen develops. Also in agreement

with this conclusion is the evidence that, aside from the targeted DC-containing region, a thorough genome-wide analysis of the WGS data did not reveal any additional genetic difference between the WT and the SS14-DC^{KO} strains, ruling out that growth in absence of the host response, or the *in vivo* attenuated phenotype of the SS14-DC^{KO} strain could be due to "background" mutations. Evidence that the *tprK* mRNA level (Fig.3B) is not affected *in vitro* by DCs ablation in the mutant strain was expected due to the significant distance (~175 kbp) between the *kan*^{R} insertion site and the *tprK* expression site. This evidence further supports that the attenuated dermal lesion phenotype was not due to impaired expression of a hypothetically essential gene. The lack of polar transcriptional effects due to the insertion of the *kan*^{R} cassette was anticipated, as the suicide vector to ablate the DCs was designed to introduce the transgene in the reverse orientation with respect to *tp0131*, the gene downstream of the DCs. *tp0131* (*tprD*) encodes a putative OMP porin, and it possibly has a critical role in *T. pallidum* biology, albeit only partially explored. Therefore, altering the expression of this gene could be detrimental to the pathogen fitness in the host. Although the location of the *tp0131* (*tprD*) promoter is uncertain, this promoter is certainly not within the deleted DC region, as the *tprD* gene in an inverted orientation compared to *kan*^{R}. Transcription of the *kan*^{R} gene past the transgene could have hypothetically generated an interfering RNA from the *tp0131* non-coding strand. However, the comparison of transcription levels attained using either RE or GSPs (Fig.3H) did not support this scenario. These data would agree with the presence of a transcription terminator immediately downstream of the *kan*^{R} cassette within the *tp0131* non-coding strand, (with sequence GGAGAAACCAG<u>GGGCAT</u>AGCGA<u>GTGTCC</u>TTTTCTGAATAG; stem nucleotides underlined) predicted *in silico* by Erpin and RNAmotif (http://rssf.i2bc.paris-saclay.fr/toolbox/arnold/index.php). This terminator is possibly responsible for ending

transcription from the resistance cassette promoter. More comprehensive mRNA sequencing studies using the WT and SS14-DC^{KO} strains propagated both *in vitro* and *in vivo* before immune clearance are currently ongoing to evaluate possible differences in these strains' global transcriptome.

Previous studies also determined that not all *T. pallidum* strains share the same repertoire of DCs and that, even within the Nichols strain, there are lineages missing a portion of the DCs contained in the region downstream of the *tprD* gene (15). Although the minimum number of DCs necessary for *T. pallidum* to maintain its full virulence is still undetermined, our results showed that that the two remaining DCs downstream of *tp0136* in the SS14-DC^{KO} strain were not sufficient to rescue the attenuated phenotype. In our study, these two sites did not appear to have contributed to the generation of new TprK variants, suggesting that their role in antigenic variation might be marginal or that variation in V7 might have a role during late-stage infection, rather than earlier. Past studies that analyzed the DC molecular architecture to define in which V region a given DC would preferentially recombine into (15, 16, 34), supported the specificity of the two residual DCs in the SS14-DC^{KO} for V7. Although more studies are needed to evaluate the importance of these isolated cassettes in generating new TprK variants, it would be plausible to assume that limited generation of variability within one single V region would not fully compensate for lack of variability in all remaining TprK V regions.

A limitation of this study could be seen in the fact that rabbits in both groups were not infected with strains completely isogenic for TprK but rather with a pathogen population carrying very few dominant TprK variants and several low-prevalence variants identified by deep sequencing. This experimental design, however, allowed us to appreciate how underrepresented variants can expand as the more abundant ones are preferentially targeted and

474 cleared during infection by the host response. We are nonetheless deriving a SS14-DC^{KO} strain
475 fully isogenic for TprK to evaluate the hypothesis that, upon ID infection with this strain, early
476 disease manifestations will be even more accentuated compared to the present study. The
477 derivation of a clonal strain will also help shed light on the role of the two residual DCs for *tprK*
478 present in the SS14-DC^{KO} genome. Although these two DCs do not seem to contribute to
479 diversity generation according to the results of this initial study, the possibility of removing the
480 genomic region harboring these residual sequences will need to be considered for future
481 experiments if evidence that recombination in V7 occurs in the mutant strain.

482 The sensitivity of the RIT assay, albeit recently questioned (35), is known to be very
483 high, with a 50% infectious dose of 23 spirochetes (36, 37). The lack of seroconversion of RIT
484 rabbits injected with lymph node extracts obtained at both day 44 and 79 from rabbits infected
485 ID with the SS14-DC^{KO} strain is intriguing, particularly if we consider that full treponemal
486 clearance was not supported by qPCR on samples collected at both time points at which the RIT
487 was performed. However, one could hypothesize that the significant reduction of the treponemal
488 burden seen in dermal lesions would necessarily translate in an abatement of the number of
489 treponemes that had disseminated to the lymph nodes to a number below the sensitivity of the
490 RIT assay. It is also possible that qPCR was detecting genomic DNA from dead treponemes.
491 This hypothesis would be supported not only by the RIT results, but also by the evidence that
492 *tprK* profiling, which requires amplification of the *tprK* coding sequence, was generally not
493 attainable in samples obtained after day 40 from rabbits infected with the SS14-DC^{KO}. In the
494 future, we will also collect biopsy specimens for RNA extraction and quantification as a
495 surrogate of treponemal viability and to assess the presence of viable treponemes by inoculating
496 Sf1Ep cultures *in vitro*. In this context, an isogenic strain would also help us understand more

clearly whether the host response cleared the SS14-DC^{KO} treponemes during infection upon performing the RIT assay. Regardless, evidence that the test animals remained RIT negative, when all the control animals developed orchitis or seroconverted, further supports the attenuation phenotype of the SS14-DC^{KO} strain.

A model for the attenuated phenotype exhibited by the mutant strain could be hypothesized on the evidence that following rabbit ID infection, inoculum SS14-DC^{KO} treponemes started to be cleared early after inoculation. By day 9, lesion development and treponemal burden in the skin tissue biopsies started to diverge significantly between the test and control rabbits (Fig.4A and Fig.5A). Within a few weeks, treponemal antibodies (including to TprK) had started to develop (Fig.5D; Fig.7D-F) and possibly contributed to clearance of WT treponemes expressing the most abundant TprK inoculum sequences (Fig.7A-C). Nonetheless, WT treponemes could still expand (Fig.5A) through the generation of new variants or the expansion of low-frequency ones in the inoculum (Fig.6, and Fig.S1-S6). In rabbits infected with the SS14-DC^{KO} strain, however, treponemal burden increase was likely hindered by the lack of DCs, even though underrepresented variants could still expand (Fig.6, and Fig.S1-S6, and Table S2) and maintain a very low pathogen burden over time (Fig.5A). Abundant *tprK* inoculum sequences in the SS14-DC^{KO} treponemes were virtually absent by day 41 post-inoculation (Fig.7G-I), even though the delayed immunity that developed to the infection in these animals likely made the antibodies responsible for clearance detectable only at later time points post-infection (Fig.7J-L). Future experiments will evaluate whether immunosuppression of the animals prior to infection would rescue the attenuation phenotype exhibited by the SS14-DC^{KO} strain.

Conclusions

We demonstrated that when genetically altered to impair its ability to vary the TprK antigen, the *T. pallidum* SS14 strain induces attenuated disease manifestations and is unable to proliferate in the rabbit model of ID infection as effectively as the WT strain. This work further supports the importance of TprK for *T. pallidum* virulence and emphasizes how our newly developed genetic engineering approach can contribute to shed light on the molecular mechanisms behind syphilis pathogenesis.

Materials and Methods

Ethics statement

Male NZW rabbits (*Oryctolagus cuniculus*) ranging from 3.5-4.5 kg in weight were purchased from Western Oregon Rabbit Company (Philomath, OR) and housed at the Harborview Medical Center – Research and Training Building vivarium. Care was provided in accordance with the Guide for the Care and Use of Laboratory Animals (38). All procedures involving these animals were approved by the UW Institutional Animal Care and Use Committee (IACUC; Protocol # 4243-01, PI: Lorenzo Giacani). Upon arrival, rabbits were allowed to acclimate to the vivarium for several days, then bled and tested with both a treponemal (*Treponema pallidum* particle agglutination, TPPA; Fujirebio, Tokyo, Japan) and a non-treponemal (Venereal Disease Research Laboratory, VDRL; Becton Dickinson, Franklin Lakes, NJ) test to confirm lack of previous or current infection with the agent of rabbit syphilis, *Treponema paraluiscuniculi*. Both tests were performed according to the manufacturer`s instructions. Only seronegative rabbits were used for experimental infection with the SS14-DC^{KO}

and SS14 parent strains (see paragraph below for rabbit infection). Rabbit rooms in the vivarium are permanently kept at 65˚F. Animals were only given antibiotic-free food and water.

TprK structure modeling

We used the ColabFold interface (39) to construct Multiple Sequence Alignments (MSA) for the TprK query sequences by searching UniRef30 (40), Mgnify (41) and ColabFold sequence databases with MMSeq2 (42). The MSA was used as input for structure prediction with AlphaFold2 (43) using the default settings (template=False, amber relax=False, 3 recycles). Increasing the number of recycles to 6 did not significantly improve the prediction. Visualization was performed using PyMol software (https://pymol.org) (44).

Suicide vector construction

The pUC57 vector (Genscript, Piscataway, NJ) was engineered to carry the *kan*^{R} gene downstream of the promoter and ribosomal binding site (RBS) of the *T. pallidum tp0574* gene (encoding the Tp47 lipoprotein) as described by Weigel *et al.* (45). An 8-nt spacer separated the RBS and the start codon of the *kan*^{R} gene. The *kan*^{R} gene sequence was derived from the Rts1 plasmid originally isolated from *Proteus vulgaris* (46) and chosen because the CDC STI treatment guidelines do not recommend the use of kanamycin for syphilis therapy. Codon optimization of the *kan*^{R} gene was shown not to be necessary in a previous study (24).

Two homology arms corresponding to the regions flanking the 51 DCs located downstream of the *tprD* gene were cloned to the left and right of the *tp0574* promoter-*kan*^{R} hybrid sequence in the pUC57 vector, respectively. The upstream and downstream arms were 990 bp and 965 bp in length, respectively, and corresponded to position 149,425-148,434 and 152,401-153,366 of the SS14 genome.

The construct was cloned between the EcoRV and KpnI sites of the pUC57 vector, in reverse orientation compared to the *lac* promoter upstream of the polylinker. Prior to use, the insert underwent Sanger sequencing to ensure sequence accuracy. The sequence of the insert is provided in File S2. This construct was named p*DC*arms-47p-*kan*^{R}. Primers annealing a) to the vector only, b) within the cloned insert, and c) upstream of the DCs homology arms in the *T. pallidum* genome are reported in Table 1. Previous work confirmed that sequences flanking the *bla* gene (encoding a β-lactamase) of the pUC57 did not carry sufficient homology to *T. pallidum* DNA to induce recombination and integration of the *bla* gene into *T. pallidum* genome (24).

To obtain a highly concentrated, endotoxin-free plasmid preparation, the p*DC*arms-47p-*kan*^{R} was transformed into TOP10 *E. coli* cells (Thermo Fisher, Waltham, MA), which were then grown first in a 5-ml starter culture overnight, and then in 500 ml of LB media supplemented with 100 µg/ml of ampicillin at 37□C. The plasmid

was purified using the Endo-Free Plasmid Mega Kit (Qiagen, Germantown, MD) according to the manufacturer's instructions. Following purification, plasmid concentration was assessed using an ND-1000 spectrophotometer (Nanodrop Technologies, Wilmington, NC). The purified vector was then aliquoted and stored at -20°C until use.

Source of *T. pallidum* for *in vitro* cultivation, transformation, and selection

The SS14 parent strain of *T. pallidum* used for *in vitro* propagation was obtained from a frozen stock previously propagated via intratesticular (IT) infection in NZW rabbits as previously reported (47). The SS14 strain was selected as a representative of the members of a globally dominant cluster, known as the SS14 clade (48). *In vitro* strain co-culturing with rabbit Sf1Ep cells was performed as per published protocols in a 6-well culture plate (Corning Inc,

588 Corning, NY) (49). Before the addition of the treponemal cells, Sf1Ep cells were incubated in a
589 5% CO_2 atmosphere in a HeraCell 150 incubator (Thermo Fisher). Following treponemal cell
590 inoculation, the microaerophilic atmosphere (MA; 1.5% O_2, 3.5% CO_2, and 95% N_2) necessary to
591 maintain treponemal viability was generated in a Heracell VIOS 160i tri-gas incubator (Thermo
592 Fisher).

593 For transformation, treponemes were first sub-cultured into the wells of a 24-well plate as
594 previously reported (24). Briefly, the day before treponemal inoculation, a 24-well plate was
595 seeded with $2x10^4$ rabbit Sf1Ep cells/well in 2.5 ml of culture media. The plates were then
596 incubated overnight in the HeraCell incubator. On the same day, TpCM-2 media was prepared
597 according to protocol and equilibrated overnight at 34°C in the tri-gas incubator. The following
598 day, cell culture media was removed from the 24-well plate, and cells were rinsed with TpCM-2
599 media equilibrated in the tri-gas incubator. Subsequently, each well was filled with 2.5 ml of
600 equilibrated TpCM-2 media, and the plate was transferred to the tri-gas incubator. To prepare the
601 treponemal inoculum, the Sf1Ep cells seeded the previous week with the parent SS14 cells were
602 trypsinized to allow the release and counting of spirochetes using an Optiphot 2 dark-field
603 microscope (DFM; Nikon, Melville, NY). Treponemal counting was performed according to
604 Lukehart and Marra (50). A total of ~$2.5x10^8$ treponemes were inoculated 24 hours after plating
605 the Sf1Ep. Following treponemal addition, the total volume of media in each well was brought to
606 2.5 ml. Two days following treponemal cell addition, 1 ml of old medium was replaced with
607 fresh medium. Four days after treponemal cell inoculation, the culture media was removed
608 gently so as not to disturb adherent treponemes. Media was replaced by 500 µl of transformation
609 buffer (50 mM $CaCl_2$, 10 mM Tris pH 7.4; equilibrated in MA) containing 15 µg total of
610 p*DC*arms-47p-*kan*^{R} vector. Cells were incubated in transformation buffer for 10 min at 34°C in

the tri-gas incubator and then washed twice with equilibrated TpCM-2 media to remove free plasmid from the culture wells. Finally, 2.5 ml of fresh TpCM-2 equilibrated in tri-gas were added to the wells, and plates were returned to the tri-gas incubator. The following day, concentrated tissue-culture grade liquid kanamycin sulfate (Sigma-Aldrich, St. Louis, MO) was added to the appropriate wells to reach a final concentration of 200 µg/ml. As a control, to confirm the treponemicidal activity of kanamycin, WT treponemes were also incubated in fresh TpCM-2 media containing kanamycin. Previous work (24) demonstrated lack of toxicity associated to $CaCl_2$ exposure for treponemes, and a $CaCl_2$ only control was not performed here again. The parent SS14 strain, however, was propagated in parallel to the transformed treponemes as a control. Kanamycin-containing TpCM-2 media was exchanged weekly but treponemes were sub-cultured every two weeks as already described (24) until they reached a density of ~10^7 cells/ml determined by DFM. At this point, cultures were sub-cultured first into one well of a 6-well plate (seeded with 10^5 Sf1Ep cells on the previous day) and then into all the wells of a 6-well plate at the following passage to further expand the strain and minimize the chances of culture loss due to contamination. At selected passages, residual treponemes were pelleted by centrifugation at 15,000 rpm for 10 min on a tabletop centrifuge and resuspended in 1X DNA lysis buffer (10 mM Tris-HCl, 0.1 M EDTA, 0.5% SDS) for DNA extraction, or Trizol (Thermo Fisher) for RNA extraction. A WT SS14 strain with limited TprK variability was attained through *in vitro* cultivation of treponemes following limiting dilution (49).

DNA and RNA extraction

DNA extraction from cultured SS14-DC^{KO} or WT strains propagated *in vitro* following the transformation procedure as well as from lesion biopsies (see below paragraph about rabbit

infection and sample collection) was performed using the QIAamp DNA Mini Kit (Qiagen) or the Zymo Quick-DNA 96 Kit (Zymo Research, Irvine, CA), respectively, according to the manufacturer's instructions. Extracted DNA was stored at -80°C until use for qualitative/quantitative amplifications or genome sequencing (see below paragraphs) to evaluate successful insertion of the *kan*^{R} gene or to evaluate treponemal burden. Samples for RNA extraction were processed according to the Trizol reagent manual. Total RNA was treated with DNaseI according to the protocol provided with the TURBO DNA-free kit (Thermo Fisher). DNA-free RNA was checked for residual DNA contamination by qualitative amplification using primers specific for the *tp0574* gene (primers in Table 1) as already described (51). Reverse transcription (RT) of total RNA was performed using the High-Capacity cDNA Reverse Transcription kit (Thermo Fisher) with random hexamers or gene-specific primers (Table 1) according to the provided protocol. cDNA samples were stored at -80°C until use for qPCR to quantify the level of expression of the *tprK* gene as previously reported (52), and the *tp0131* (*tprD*) gene, also as reported (53). All transcripts were normalized to the *tp0574* expression level (primers in Table 1).

Droplet digital PCR (ddPCR)

Droplet digital PCR assays were conducted to assess the ratio between the number of copies of the *kan*^{R} gene, the *tp0001* gene (*dnaA*), and an open reading frame (ORF; *tp0127*) encoding a 229 amino acid-long hypothetical protein with unknown function contained within the ablated DCs region. This short ORF was selected because it is unique to the ablated region, while primers annealing directly to the DCs sequences could potentially also recognize sequences in the *tprK* expression site. Analyzed DNA was extracted from the SS14-DC^{KO} from

in vitro passages 2-5 post-transformation and from the parent SS14 strain propagated in parallel. ddPCR was performed on a Bio-Rad QX100 system (Bio-Rad, Carlsbad, CA). Primers and probe are listed in Table 1. Each reaction was performed using ddPCR Supermix for Probes (Bio-Rad) with the final concentration of primers at 900 nM and probes at 250 nM in a total reaction volume of 25 µl. Before amplification, template DNA was digested with 25 units of EcoRI (New England Biolabs, Ipswich, MA). After droplet generation, droplets were transferred to a 96-well PCR plate and amplified on a 2720 Thermal Cycler (Thermo Fisher) with the following cycling parameters: 94°C for 10 min, followed by 40 cycles of 94°C for 30 s and 60°C for 1 min, and 98°C hold for 10 min. After amplification, the plate was transferred to QX200 droplet reader (Bio-Rad). Results were analyzed using the QuantaSoft software (Bio-Rad).

T. pallidum whole-genome sequencing

Whole-genome sequencing was performed following DNA extraction of SS14-DC^{KO} cultured *in vitro* and harvested at passage #9 post-transformation. Pre-capture libraries were prepared from up to 100 ng input DNA using the KAPA Hyperplus kit (Roche) and TruSeq adapters and barcoded primers (Illumina), following the manufacturer's protocols, yielding an average library size longer than 400 bp. Hybrid capture of *T. pallidum* genomic DNA was performed overnight (>16 hours) using a custom IDT xGen panel designed against the reference genome NC_010741, following the manufacturer's protocol. Short-read sequencing was performed on an Illumina NextSeq 2000 with 150 bp paired-end reads, yielding 2.75 and 8.20 million raw reads for WT and mutant strains, respectively. Reads were adapted and quality trimmed using Trimmomatic v0.39 (54) and assembled to the *T. pallidum* SS14 reference genome NC_021508.1, or NC_021508.1 with the DC region manually replaced by the *kan*^{R}

cassette, using Bowtie2 v2.4.1 (55) and deduplicated with Picard MarkDuplicates v2.23.3 (available at http://broadinstitute.github.io/picard), to an average coverage exceeding 177x for the WT and 405x for the KO strain. Manual confirmation of expected coverage and junctions was performed by visual inspection in Geneious Prime v2020.1.2 (56). Raw reads were deposited to the NCBI Sequence Read Archive under BioProject PRJNA909291.

Qualitative and quantitative PCR

Samples harvested during routine propagation of the SS14-DC^{KO} and parent strains were assessed for integration of the *kan*^{R} gene into the DC locus by using qualitative PCR. All primers used in these assays and amplicon sizes are reported in Table 1. In the first amplification, the sense primer targeted a region of the *T. pallidum* genome immediately upstream of the left homology arm of the vector (and hence not cloned into p*DC*arms-47p-*kan*^{R}), while the antisense primers targeted the *kan*^{R} gene, with the rationale that only a *kan*^{R} gene integrated into the DC region would provide amplification. In the second PCR, the sense primer targeted the *kan*^{R} gene, and the antisense primer targeted the genomic region downstream of the right homology arm of the vector. A third PCR used both primers external to the homology arms to show a differential in size when DNA from the transformed and parent strain, respectively, was used. Amplification of the *tp0574* gene was used as positive amplification control, and amplification with pUC57 plasmid-specific primers was performed to confirm that no residual transformation plasmid persisted in the SS14-DC^{KO} culture. Amplifications were performed using five microliters of extracted DNA in 50 µl final volume containing 2.5 units of GoTaq polymerase (Promega, Madison, WI), 200 µM of each dNTP, 1.5 mM of $MgCl_2$, and 400 nM of sense and antisense primers. Cycling parameters were initial denaturation (94°C) and final extension (72°C) for 10

min each. Denaturation (94°C) and annealing (60°C) steps were carried on for 1 min each, while the extension step (72°C) was carried out for 1 or 2 min depending on amplicon length. A total of 40 cycles were performed in each reaction.

A TaqMan qPCR assay targeting the *tp0574* gene was instead used to quantify treponemal load in samples extracted from rabbit lesion biopsies as previously described (57). Primers/probe and amplicon size are reported in Table 1. Amplifications were run on a QuantStudio 3 or 5 thermal cycler (Thermo Fisher) and results were analyzed using the instrument software. Data were imported into Prism 8 (GraphPad Software, San Diego, CA) and further analyzed to assess statistical significance of the values from the control rabbits and those infected with the knockout strain using one-way ANOVA with the Dunnett test for correction of multiple comparisons or Student's *t*-test, with significance set at $p<0.05$ in both cases.

TprK molecular profiling

TprK libraries were prepared similarly as previously described (17). Technical duplicates were performed with thirty-five cycles of PCR in a 50 μL reaction with 0.4 mM TprK forward and reverse primers (Table S4) using the 2x CloneAmp MasterMix (Takara) with a 62°C annealing temperature. Biopsy DNA input was limited to 4 μL per reaction due to high host DNA concentration inhibiting amplification, which represented a range of 75-1433320 genome copies. For the parent and SS14-DC^{KO} inoculum propagated *in vitro*, 1e6 genome copies were input. PCR products were run on a 1% agarose gel to confirm the presence of a band at approximately 1.6 kb and cleaned with 0.6x Ampure beads (Beckman Coulter); samples with fewer than 200 input genome copies were excluded from further analysis due to inconsistent amplification. Two nanograms of PCR product were used in a two-fifths Nextera (Illumina)

library prep with 15 cycles of amplification. Low molecular weight products were removed with 0.6x Ampure beads, with an average size of approximately 350 bp. Libraries were quantified, pooled, and run on a 2x150 paired end run on an Illumina Nextseq 2000. Raw reads were adapter-trimmed and filtered for quality scores above Q20 using Trimmomatic v0.39 (54), followed by merging the paired end reads using BBmerge (https://www.osti.gov/biblio/1241166) in default parameters. Variable site sequences were identified using custom python and R scripts (22), and those containing frameshifts or nonsense mutations in the translated sequences removed. Replicate samples yielding a minimum of 2,000 reads in all V regions in both replicates were kept for downstream analysis, corresponding to input merged reads ranging between 89182–5746195. Only sequences with 5 or more raw reads per technical replicate were retained per sample. Samples with a Pearson correlation coefficient lower than 0.95 between replicates were removed, and the number of reads for each variable region in each technical replicate were averaged. Sequences with less than 0.25% prevalence per V region per sample were excluded from further analysis. Raw reads are available in NCBI BioProject PRJNA909291.

Rabbit intradermal infection, lesion monitoring, and sample collection

Two groups of 4 animals each were infected intradermally (ID) on the same day on ten sites/animal on their shaved backs with 10^6 viable *T. pallidum* cells. One group received the WT SS14 strain, and the other group was infected with the SS14-DC^{KO} strain. Briefly, the day of the ID infection, treponemes were harvested from culture plates as described above for routine passages. Following a low speed-centrifugation for 10 min at 1,000 rpm in a R4702 centrifuge (Eppendorf, Hauppauge, NY) to remove rabbit Sf1Ep cells, treponemal cells were enumerated

and checked for motility by DFM and diluted using sterile saline to a final concentration of 10^7 cells/ml. One hundred microliters of treponemal suspension were injected in each site on the rabbit backs. Treponemal cells were evaluated again for motility using DFM after performing ID inoculation to ensure that pathogen viability was unaltered at the end of the procedure.

Intradermally-infected rabbits were shaved daily post-inoculation to allow monitoring of lesion progression and to facilitate collection of needle aspirates and lesion biopsies. Two animals from each group were euthanized on day 44 post-inoculation to harvest popliteal lymph nodes and perform an RIT (see paragraph below). The remaining four animals were monitored for an additional 36 days, and then also euthanized to perform RIT.

Lesion biopsies and aspirates were collected at day 9, 22, 30, 37, 41 post-infection from all animals, at day 44 post-infection from the four animals that were euthanized first, and at day 51, 58, 65, 72, and 79 from the remaining four animals. One biopsy per animal was obtained per collection day using a 4 mm biopsy punch. At day 44, however, biopsies were collected from all lesions (unless previously biopsied) of the animals that were euthanized to perform the first round of RIT assays. Aspirates were collected from approximately half of the lesions from each rabbit per collection day. Once biopsied, a lesion was no longer measured or used to collect aspirates. Aspirates were obtained using an Excel 1cc zero dead space tuberculin syringe with a 25Gx3/8” needle (Excel international, Birmingham, AL) by inserting the needle laterally into the side of the developing lesion. Once inserted, the plunger was drawn, and the needle moved back and forth five times while holding the plunger. Lesion aspirates were resuspended in 60 μl of sterile saline, and 18 μl of each suspension were examined by DFM to assess for the presence and number of treponemes. *T. pallidum* cells were counted blindly in a total of 50 fields/sample. The operator was blinded to the identity of the samples. Biopsies were minced using forceps and

a sterile scalpel, resuspended in 1X DNA lysis buffer. Serum was obtained weekly from each animal to perform VDRL and TPPA tests to monitor development of humoral immunity in response to infection. Statistical analyses were performed using one-way ANOVA with the Dunnett correction of multiple comparisons or Student's *t*-test, with significance set at $p<0.05$.

Rabbit infectivity test (RIT)

Immediately after euthanasia, popliteal lymph nodes were harvested from rabbits to perform an RIT as previously described (50). Following injection of minced popliteal lymph nodes in the animal's left testis, RIT rabbits were monitored twice a week for orchitis development. If orchitis developed, to ascertain that it was due to *T. pallidum* infection, testicular needle aspiration was performed as described above to be analyzed by DFM. If orchitis was confirmed by finding treponemes in the sample, then the animal was euthanized. As orchitis does not always develop in RIT animals, rabbits were also bled monthly to assess seroconversion using VDRL and TPPA tests. If seroconversion occurred, the animal was euthanized. If at the end of the 3-month observation period following IT injection, the rabbit had not developed orchitis or seroconverted, then the RIT outcome was negative, and the animal was deemed uninfected.

Rabbit intratesticular infection

To assess differences in *in vivo* growth between the parent and knockout strains studied here, one rabbit was infected IT with the *T. pallidum* parent SS14 strain ($7x10^7$ cells/testis), while a second animal was inoculated with the SS14-DC^{KO} strains IT ($6x10^7$ cells/testis). Both animals were monitored daily to determine the time to orchitis. At peak orchitis, animals were

euthanized, testes were harvested, and content extracted in 10 ml of sterile saline to quantify treponemal burden by DFM. Procedures were performed as previously described (50).

ELISA using V region synthetic peptides

Synthetic peptides were designed based upon the TprK profiling results for a subset of animals infected with the SS14-DC^{KO}. A total of 5 peptides matching inoculum sequences for both the WT and SS14-DC^{KO} strains (Table 3, labelled with a superscripted "1") were produced by Genscript (Piscataway, NJ). Upon reception, lyophilized peptides were rehydrated in sterile PBS (supplemented with DMSO or acetic-acid) to a stock solution of 4mg/ml. Reconstituted peptides were stored at -80°C until use. For ELISA, peptides were further diluted to 10 μg/ml in PBS, and 50 μl of working dilution (500 ng total) were used to coat the wells of a 96-well Microwell Maxisorp flat-bottom plate (Thermo-Fisher, Waltham, MA) as previously described (19). Briefly, plates were then washed three times with PBS+0.05% Tween-20 and blocked with 200 μl of 5% nonfat dry milk (NFM) in sterile PBS for three hours. At this step, NFM was used to block no-antigen wells for background signal. Wells were then washed again as above and primary antibody was applied immediately thereafter. Sera from infected animals were used at a 1:20 dilution. After overnight incubation with the primary antibody, plates were washed again as above and 100 μl of a goat anti-rabbit IgG (H + L) alkaline phosphatase conjugate (Sigma, St. Louis, MO) diluted 1:2,000 in PBS/1% NFM were added to each well and incubated for 1.5h at room temperature. Plates were washed again and developed with 50 μl/well of 1 mg/ml para-Nitrophenyl Phosphate (pNPP) substrate (Sigma), dissolved in glycine buffer (0.1M glycine, pH 10.4, 1mM $MgCl_2$ and 1 mM $ZnCl_2$) for 1 h according to the manufacturer`s instructions. Absorbance was measured at OD_{405} using a Molecular Devices SpectraMax Plus microplate

reader (Molecular Devices, San Jose, CA). The mean of triplicate experimental wells minus the mean of pre-infection serum wells tested with the same antigen was calculated for all proteins/peptides tested. Plotted data represent the mean ± SEM for triplicate wells tested. Results were analyzed using Student's *t*-test with significance set at $p \leq 0.05$.

Acknowledgments

This work was supported by NIAID grant number U19AI144133 (Project 2 and Genomics and Isolation Core; Project 2 leader: L.G.; Core leaders: L.G. and A.L.G.; PI: Anna Wald, University of Washington) and by Open Philanthropy (to L.G.). The content of this study is solely the responsibility of the authors and does not necessarily represent the official views of the National Institutes of Health or Open Philanthropy. The funders had no role in study design, data collection, and analysis, decision to publish, or preparation of the manuscript.

Figure Legends

Figure 1. TprK (sequence AIP85979.1) is predicted by AlphaFold2 to fold into a 20-strands beta-barrel structures with 10 surface-exposed loops. Variable loops (V1-V7) are highlighted in colour. Conserved loops (C1-C3) are in white, and β-scaffolding are in light blue. OM: outer membrane; PS: periplasmic space.

Figure 2. *In vitro* growth curves of the strains used here and molecular assessment of integration of the *kan*^{R} cassette. (**A**) Twenty-eight-week *in vitro* growth curve of transformed SS14 *T. pallidum* cells (SS14-DC^{KO}) in selective media (solid orange circles), WT SS14 cells in selective media (solid black triangles), and WT SS14 strain in non-selective media (solid blue squares).

Propagation of the parent strain for this experiment stopped at week 18. Parent treponemes propagated in kanamycin-containing media were never countable by DFM. (**B; subpanels 1-5**) Qualitative amplifications to assess *kan*^{R} integration. Primer combinations are reported in Table 1. Subpanels show amplifications a) with vector-specific primers (subpanel #1, 2,967 bp amplicon), yielding an amplicon only with suicide vector control DNA; b) with *tp0574* primers (subpanel #2, 313 bp amplicon), positive in both parent and transformed treponemes; c) with primers annealing to the *kan*^{R} gene and outside of the right homology arm in the *T. pallidum* genome (subpanels #3; 1,846 bp size amplicon), yielding a positive amplicon only with template from transformed treponemes; d) with primers annealing upstream and downstream of the homology arms in the *T. pallidum* genome (subpanel #4, 2,982 bp and 5,980 bp size amplicons), yielding a shorter amplicon size in transformed treponemes due to deletion of the DCs); and primers annealing to the *kan*^{R} gene (subpanel #5, 663 bp size amplicon). M: molecular size marker (bp); KO: SS14-DC^{KO}, WT: parent WT SS14; NTC: No-template control, P: suicide vector (p*DC*arms-47p-*kan*^{R}) plasmid DNA.

Figure 3. Confirmation of *kan*^{R} cassette integration using ddPCR and WGS, and message quantifications. **(A)** Ratios between the *kan*^{R}, *dnaA (tp0001)*, and *tp0127* (contained within the deleted DC) copy number determined by droplet digital PCR (ddPCR) on template DNA from the SS14-DC^{KO} and parent SS14 strain harvested at passage #2-5 post-transformation. The *kan*^{R}:*dnaA* ratio for the parent SS14 was zero at each passage. **(B)** Message quantification of *tprK* (normalized to *tp0574*) in SS14-DC^{KO} and parent SS14 strain propagated *in vitro* showing comparable expression of *tprK* between the control and transformed strain. Significance ($p<0.05$) was assessed by performing Student's *t*-test. **(C-G)** Whole-genome sequencing of the SS14-

DC^{KO} and WT strains (passage #9) post-transformation. (**C**) SS14-DC^{KO} reads assembled to the WT genome reference (NC_021508.1/CP004011.1) showing a gap where the DC locus previously was. **(D)** SS14-DC^{KO} reads assembled to the SS14-DC^{KO} reference genome, where the DC locus was replaced *in silico* with the *kan*^{R} cassette sequence showing reads aligning to the cassette sequence. **(E)** Schematic of the 51 deleted DCs, color-coded based on their target V region and the *kan*^{R} cassette (*tp0574* promoter- *kan*^{R}) that replaced the DCs. **(F)** Reads from the WT SS14 genome aligned to the SS14 reference genome showing the integrity of the DC locus. (**G**) Reads from the WT genome aligned to the SS14-DC^{KO} reference genome showing a gap where the *kan*^{R} cassette is located. (**H-I**) Messsage quantification of the *tp0131* and *kan*^{R} genes in the WT and the SS14-DC^{KO} strain showing lack of transcriptional polar effects due to the substitution of the DCs. mRNA was reverse-transcribed using either gene-specific primers (GSP, white bars) or random hexamers (RE; black bars); ns: not significant.

Figure 4. Lesion progression in infected animals. **(A)** Measurements of lesion diameter (mm) over time in rabbits infected with the SS14 strain and the SS14-DC^{KO} strain. Statistical analyses were performed using one-way ANOVA with the Dunnett correction of multiple comparisons or Student's *t*-test, with significance set at $p<0.05$, indicated by an asterisk. The designation "ns" indicates lack of significance in lesion diameter of rabbits infected with the WT strain between day 65 and subsequent time points. **(B)** Pictures of the animals still in the study at day 72 post-infection showing large, ulcerated lesions in control rabbits (right panel), and significantly smaller ($p<0.05$) lesions in animals infected with the knockout strain (left panel). Circled areas represent lesions that were not yet biopsied at the time the picture was taken. Black ink dots near the lesion area mark the injection sites.

Figure 5. Treponemal burden and serologies of infected animals. **(A)** Treponemal burden in lesion biopsies collected from control and test animals assessed by qPCR targeting the *tp0574* gene. The presence of *T. pallidum* DNA was confirmed in all samples, but treponemal burden in control samples was uniformly higher. Statistical analyses were performed using Student's *t*-test, with significance set at $p<0.05$ ($p<0.01$ is indicated with two asterisks, $p<0.001$ is indicated with three asterisks). **(B)** Treponemal burden in lesion biopsies collected from control and test animals assessed by DFM in lesion needle aspirates. Treponemes could be detected only in samples from control rabbits. **(C)** Significant delay in development of VDRL antibody titers in sera collected from animals infected with the knockout strain compared to serum samples from control rabbits. Controls seroconverted earlier and achieved significantly higher titers compared to test animals. Uninfected rabbit sera (screened at animal arrival at the vivarium) pre-inoculation had no VDRL reactivity. **(D)** Initial delay in development of treponemal antibodies (assessed using the TPPA test) in test animals compared to control rabbits. Titer differences became not significant at day 30 post-inoculation. NR: Nonreactive. In both cases significance ($p<0.05$) was assessed by performing Student's *t*-test. Uninfected rabbit sera (screened at animal arrival at the vivarium) pre-inoculation had no TPPA reactivity.

Figure 6. Heatmap of sequence diversity in TprK V6**.** Amino acid sequences of TprK V6 derived from SS14-WT (left) or SS14-DC^{KO} (right), separated by a bold dotted line. Each column represents the sequences present in a single biopsy for a single animal at a particular timepoint, with biopsy timepoints arranged left to right and animals separated by light dotted lines. Color scale represents the prevalence of each amino acid sequence within each sample.

Inoculum samples are labeled "Inoc". Sequences are arranged in order of decreasing prevalence in SS14-DC^{KO} inoculum, then by SS14-WT inoculum. Missing samples did not yield data. Interactive heatmaps are available at https://github.com/greninger-lab/Impaired-TprK-Antigenic-Variation. Peptide sequences and prevalence are also reported in Table S2.

Figure 7. Comparison between changes over time in sequence abundance of selected V5 and V6 regions present in the inoculum treponemes and the development of humoral immunity to the same regions, assessed by ELISA performed with sera from infected rabbits and synthetic peptides. Panels A-C (sequence abundance) and D-F (humoral response to the selected peptide) pertain to rabbits infected with the WT strain, while panels G-I (sequence abundance) and J-L (humoral response to the selected peptide) pertain to rabbits infected with the SS14-DC^{KO} strain. Sequence abundance was based on the *tprK* deep sequencing results for all rabbits.

Figure S1. Heatmap of sequence diversity in TprK V1. Deep sequencing of TprK V1 region showing persistence of inoculum variants and generation of non-inoculum variants in samples collected overtime from rabbits infected with the WT SS14 strain ("WT"-labeled samples, left side of the map) and form rabbits infected with the SS14-DC^{KO} strain ("KO"-labeled samples, right side of the map), separated by a bold vertical dashed line. In each map, inoculum sequences for the WT strain are labeled as "WT Inoc B00 Day 00", where WT Inoc indicates WT inoculum treponemes, B00 indicates that the sample was not obtained from a biopsy, and Day 00 indicates the experiment's time 0. The same nomenclature was adopted for the SS14-DC^{KO} inoculum, with the exception that KO replaced WT. Samples collected post-inoculation report rabbit number (R#), biopsy number (B#), and day post-inoculation the sample was obtained (Day#). Light gray

dashed lines separate individual animals. Missing samples did not yield data. The same heatmap in interactive format is available at https://github.com/greninger-lab/Impaired-TprK-Antigenic-Variation. Peptide sequences and prevalence are also reported in Table S2.

Figure S2. Heatmap of sequence diversity in TprK V2. Deep sequencing of TprK V2 region showing persistence of inoculum variants and generation of non-inoculum variants in samples collected overtime from rabbits infected with the WT SS14 strain ("WT"-labeled samples, left side of the map) and form rabbits infected with the SS14-DC^{KO} strain ("KO"-labeled samples, right side of the map), separated by a bold vertical dashed line. In each map, inoculum sequences for the WT strain are labeled as "WT Inoc B00 Day 00", where WT Inoc indicates WT inoculum treponemes, B00 indicates that the sample was not obtained from a biopsy, and Day 00 indicates the experiment's time 0. The same nomenclature was adopted for the SS14-DC^{KO} inoculum, with the exception that KO replaced WT. Samples collected post-inoculation report rabbit number (R#), biopsy number (B#), and day post-inoculation the sample was obtained (Day#). Light gray dashed lines separate individual animals. Missing samples did not yield data. The same heatmap in interactive format is available at https://github.com/greninger-lab/Impaired-TprK-Antigenic-Variation. Peptide sequences and prevalence are also reported in Table S2.

Figure S3. Heatmap of sequence diversity in TprK V3. Deep sequencing of TprK V3 region showing persistence of inoculum variants and generation of non-inoculum variants in samples collected overtime from rabbits infected with the WT SS14 strain ("WT"-labeled samples, left side of the map) and form rabbits infected with the SS14-DC^{KO} strain ("KO"-labeled samples, right side of the map), separated by a bold vertical dashed line. In each map, inoculum sequences

for the WT strain are labeled as “WT Inoc B00 Day 00”, where WT Inoc indicates WT inoculum treponemes, B00 indicates that the sample was not obtained from a biopsy, and Day 00 indicates the experiment’s time 0. The same nomenclature was adopted for the SS14-DC^{KO} inoculum, with the exception that KO replaced WT. Samples collected post-inoculation report rabbit number (R#), biopsy number (B#), and day post-inoculation the sample was obtained (Day#). Light gray dashed lines separate individual animals. Missing samples did not yield data. The same heatmap in interactive format is available at https://github.com/greninger-lab/Impaired-TprK-Antigenic-Variation. Peptide sequences and prevalence are also reported in Table S2.

Figure S4. Heatmap of sequence diversity in TprK V4. Deep sequencing of TprK V4 region showing persistence of inoculum variants and generation of non-inoculum variants in samples collected overtime from rabbits infected with the WT SS14 strain (“WT”-labeled samples, left side of the map) and form rabbits infected with the SS14-DC^{KO} strain (“KO”-labeled samples, right side of the map), separated by a bold vertical dashed line. In each map, inoculum sequences for the WT strain are labeled as “WT Inoc B00 Day 00”, where WT Inoc indicates WT inoculum treponemes, B00 indicates that the sample was not obtained from a biopsy, and Day 00 indicates the experiment’s time 0. The same nomenclature was adopted for the SS14-DC^{KO} inoculum, with the exception that KO replaced WT. Samples collected post-inoculation report rabbit number (R#), biopsy number (B#), and day post-inoculation the sample was obtained (Day#). Light gray dashed lines separate individual animals. Missing samples did not yield data. The same heatmap in interactive format is available at https://github.com/greninger-lab/Impaired-TprK-Antigenic-Variation. Peptide sequences and prevalence are also reported in Table S2.

Figure S5. Heatmap of sequence diversity in TprK V5. Deep sequencing of TprK V5 region showing persistence of inoculum variants and generation of non-inoculum variants in samples collected overtime from rabbits infected with the WT SS14 strain ("WT"-labeled samples, left side of the map) and form rabbits infected with the SS14-DC^{KO} strain ("KO"-labeled samples, right side of the map), separated by a bold vertical dashed line. In each map, inoculum sequences for the WT strain are labeled as "WT Inoc B00 Day 00", where WT Inoc indicates WT inoculum treponemes, B00 indicates that the sample was not obtained from a biopsy, and Day 00 indicates the experiment's time 0. The same nomenclature was adopted for the SS14-DC^{KO} inoculum, with the exception that KO replaced WT. Samples collected post-inoculation report rabbit number (R#), biopsy number (B#), and day post-inoculation the sample was obtained (Day#). Light gray dashed lines separate individual animals. Missing samples did not yield data. The same heatmap in interactive format is available at https://github.com/greninger-lab/Impaired-TprK-Antigenic-Variation. Peptide sequences and prevalence are also reported in Table S2.

Figure S6. Heatmap of sequence diversity in TprK V7. Deep sequencing of TprK V7 region showing persistence of inoculum variants and generation of non-inoculum variants in samples collected overtime from rabbits infected with the WT SS14 strain ("WT"-labeled samples, left side of the map) and form rabbits infected with the SS14-DC^{KO} strain ("KO"-labeled samples, right side of the map), separated by a bold vertical dashed line. In each map, inoculum sequences for the WT strain are labeled as "WT Inoc B00 Day 00", where WT Inoc indicates WT inoculum treponemes, B00 indicates that the sample was not obtained from a biopsy, and Day 00 indicates the experiment's time 0. The same nomenclature was adopted for the SS14-DC^{KO} inoculum, with the exception that KO replaced WT. Samples collected post-inoculation report rabbit number

(R#), biopsy number (B#), and day post-inoculation the sample was obtained (Day#). Light gray dashed lines separate individual animals. Missing samples did not yield data. The same heatmap in interactive format is available at https://github.com/greninger-lab/Impaired-TprK-Antigenic-Variation. Peptide sequences and prevalence are also reported in Table S2.

File S1. Sequence of the insert (yellow/green/gray bases) contained in the p*DC*arms-47p-*kan*^{R} suicide vector built using a pUC57 plasmid backbone, flanking regions (aqua), and primers used to evaluate the replacement of the DCs in the transformed *T. pallidum* strain.

Table S1. TprK variability profile in the WT SS14 and SS14-DS^{KO} strains used for rabbit inoculation. Highly represented sequences (>10% of the total) are in bold.

Table S2. Results of the TprK profiling showing variant sequences with ≥0.25% prevalence for each V region, time point, and infected rabbit.

Table S3. Inoculum variants detected in rabbits infected with the SS14-DC^{KO} strain at <0.25% reads. KO = rabbit infected with the DC^{KO} strain; R = rabbit#; B = biopsy#; Day# = day post-inoculation; (%) = percentage of sequence compared to all sequences detected in the sample for a given V region at this time point.

Table S4. Barcoded primers used in this study for *tprk* deep sequencing.

References

1. WHO. Prevalence and incidence of selected sexually transmitted infections *Chlamydia trachomatis, Neisseria gonorrhoeae*, syphilis and *Trichomonas vaginalis*: methods and results used by WHO to generate 2005 estimates. World Health Organization, Geneva. 2011.

2. Gerbase AC, Rowley JT, Mertens TE. Global epidemiology of sexually transmitted diseases. The Lancet. 1998;351.

3. CDC. 2018 Sexually Transmitted Disease Surveillance. Atlanta, GA: US Department of Health and Human Services: Centers for Disease Control and Prevention. 2019.

4. Savage EJ, Marsh K, Duffell S, Ison CA, Zaman A, Hughes G. Rapid increase in gonorrhoea and syphilis diagnoses in England in 2011. Euro Surveill. 2012;17(29).

5. Savage EJ, Hughes G, Ison C, Lowndes CM. Syphilis and gonorrhoea in men who have sex with men: a European overview. Euro Surveill. 2009;14(47).

6. Simms I, Fenton KA, Ashton M, Turner KM, Crawley-Boevey EE, Gorton R, et al. The re-emergence of syphilis in the United Kingdom: the new epidemic phases. Sex Transm Dis. 2005;32(4):220-6.

7. Tucker JD, Cohen MS. China's syphilis epidemic: epidemiology, proximate determinants of spread, and control responses. Curr Opin Infect Dis. 2011;24(1):50-5.

8. Jin F, Prestage GP, Kippax SC, Pell CM, Donovan BJ, Kaldor JM, et al. Epidemic syphilis among homosexually active men in Sydney. Med J Aust. 2005;183(4):179-83.

9. Goldenberg RL, Thompson C. The infectious origins of stillbirth. Am J Obstet Gynecol. 2003;189(3):861-73.

10. Moline HR, Smith JF, Jr. The continuing threat of syphilis in pregnancy. Curr Opin Obstet Gynecol. 2016;28(2):101-4.

11. Wijesooriya NS, Rochat RW, Kamb ML, Turlapati P, Temmerman M, Broutet N, et al. Global burden of maternal and congenital syphilis in 2008 and 2012: a health systems modelling study. Lancet Glob Health. 2016;4(8):e525-33.

12. Peeling RW, Mabey D, Kamb ML, Chen XS, Radolf JD, Benzaken AS. Syphilis. Nat Rev Dis Primers. 2017;3:17073.

13. LaFond RE, Lukehart SA. Biological basis for syphilis. Clin Microbiol Rev. 2006;19(1):29-49.

14. Lian T, Zhang B, Giacani L, Kou C, Yang X, Zhang R, et al. Full-length TprK of *Treponema pallidum* subsp. *pallidum* in lipid nanodiscs is a monomeric porin. Enzyme Microb Technol. 2021;153:109897.

15. Giacani L, Brandt SL, Puray-Chavez M, Brinck Reid T, Godornes C, Molini BJ, et al. Comparative Investigation of the Genomic Regions Involved in Antigenic Variation of the TprK Antigen among Treponemal Species, Subspecies, and Strains. J Bacteriol. 2012;194(16):4208-25.

16. Centurion-Lara A, LaFond RE, Hevner K, Godornes C, Molini BJ, Van Voorhis WC, et al. Gene conversion: a mechanism for generation of heterogeneity in the *tprK* gene of *Treponema pallidum* during infection. Molecular Microbiology. 2004;52(6):1579-96.

17. Addetia A, Lin MJ, Phung Q, Xie H, Huang ML, Ciccarese G, et al. Estimation of Full-Length TprK Diversity in *Treponema pallidum* subsp. *pallidum*. mBio. 2020;11(5).

18. LaFond RE, Centurion-Lara A, Godornes C, Van Voorhis WC, Lukehart SA. TprK sequence diversity accumulates during infection of rabbits with *Treponema pallidum* subsp. *pallidum* Nichols strain. Infect Immun. 2006;74(3):1896-906.

19. Morgan CA, Molini BJ, Lukehart SA, Van Voorhis WC. Segregation of B and T cell epitopes of *Treponema pallidum* repeat protein K to variable and conserved regions during experimental syphilis infection. J Immunol. 2002;169(2):952-7.

20. LaFond RE, Molini BJ, Van Voorhis WC, Lukehart SA. Antigenic variation of TprK V regions abrogates specific antibody binding in syphilis. Infect Immun. 2006;74(11):6244-51.

21. Giacani L, Molini BJ, Kim EY, Godornes BC, Leader BT, Tantalo LC, et al. Antigenic variation in *Treponema pallidum*: TprK sequence diversity accumulates in response to immune pressure during experimental syphilis. J Immunol. 2010;184(7):3822-9.

22. Lin MJ, Haynes AM, Addetia A, Lieberman NAP, Phung Q, Xie H, et al. Longitudinal TprK profiling of in vivo and in vitro-propagated *Treponema pallidum* subsp. *pallidum* reveals accumulation of antigenic variants in absence of immune pressure. PLoS Negl Trop Dis. 2021;15(9):e0009753.

23. Reid TB, Molini BJ, Fernandez MC, Lukehart SA. Antigenic variation of TprK facilitates development of secondary syphilis. Infect Immun. 2014;82(12):4959-67.

24. Romeis E, Tantalo L, Lieberman N, Phung Q, Greninger A, Giacani L. Genetic engineering of *Treponema pallidum* subsp. *pallidum*, the Syphilis Spirochete. PLoS Pathog. 2021;17(7):e1009612.

25. Giacani L, Iverson-Cabral SL, King JC, Molini BJ, Lukehart SA, Centurion-Lara A. Complete Genome Sequence of the *Treponema pallidum* subsp. *pallidum* Sea81-4 Strain. Genome Announc. 2014;2(2).

26. Falkow S. Molecular Koch's postulates applied to microbial pathogenicity. Rev Infect Dis. 1988;10 Suppl 2:S274-6.

27. Chi B, Chauhan S, Kuramitsu H. Development of a system for expressing heterologous genes in the oral spirochete *Treponema denticola* and its use in expression of the *Treponema pallidum flaA* gene. Infect Immun. 1999;67(7):3653-6.

28. Chan K, Nasereddin T, Alter L, Centurion-Lara A, Giacani L, Parveen N. *Treponema pallidum* Lipoprotein TP0435 Expressed in Borrelia burgdorferi Produces Multiple Surface/Periplasmic Isoforms and mediates Adherence. Sci Rep. 2016;6:25593.

29. Cameron CE, Kuroiwa JM, Yamada M, Francescutti T, Chi B, Kuramitsu HK. Heterologous expression of the *Treponema pallidum l*aminin-binding adhesin Tp0751 in the culturable spirochete *Treponema phagedenis*. J Bacteriol. 2008;190(7):2565-71.

30. Hazlett KRO, Sellati TJ, Nguyen TT, Cox DL, Clawson ML, Caimano MJ, et al. The TprK protein of *Treponema pallidum* is periplasmic and is not a target of opsonic antibody or protective immunity. J Exp Med. 2001;193(9):1015-26.

31. Stamm LV, Bergen HL. The sequence-variable, single-copy *tprK* gene of *Treponema pallidum* Nichols strain UNC and street strain 14 encodes heterogeneous TprK proteins. Infect Immun. 2000;68(11):6482-6.

32. Centurion-Lara A, Godornes C, Castro C, Van Voorhis WC, Lukehart SA. The *tprK* gene is heterogeneous among *Treponema pallidum* strains and has multiple alleles. Infect Immun. 2000;68(2):824-31.

33. LaFond RE, Centurion-Lara A, Godornes C, Rompalo AM, Van Voorhis WC, Lukehart SA. Sequence diversity of *Treponema pallidum* subsp. *pallidum tprK* in human syphilis lesions and rabbit-propagated isolates. J Bacteriol. 2003;185(21):6262-8.

34. Addetia A, Tantalo LC, Lin MJ, Xie H, Huang ML, Marra CM, et al. Comparative genomics and full-length Tprk profiling of *Treponema pallidum* subsp. *pallidum* reinfection. PLoS Negl Trop Dis. 2020;14(4):e0007921.

35. Tong ML, Zhang HL, Zhu XZ, Fan JY, Gao K, Lin LR, et al. Re-evaluating the sensitivity of the rabbit infectivity test for *Treponema pallidum* in modern era. Clin Chim Acta. 2017;464:136-41.

36. Turner TB, Hollander DH. Biology of the Treponematoses. Geneva: World Health Organization; 1957.

37. Turner TB, Hardy PH, Newman B. Infectivity tests in syphilis. Br J Vener Dis. 1969;45(3):183-96.

38. Janier M. Ceftriaxone is effective for treating patients with primary syphilis. Sex Transm Dis. 1988;15(1):70.

39. Mirdita M, Schütze K, Moriwaki Y, Heo L, Ovchinnikov S, Steinegger M. ColabFold - Making protein folding accessible to all. bioRxiv. 2021:2021.08.15.456425.

40. Suzek BE, Wang Y, Huang H, McGarvey PB, Wu CH. UniRef clusters: a comprehensive and scalable alternative for improving sequence similarity searches. Bioinformatics. 2015;31(6):926-32.

41. Mitchell AL, Almeida A, Beracochea M, Boland M, Burgin J, Cochrane G, et al. MGnify: the microbiome analysis resource in 2020. Nucleic Acids Res. 2020;48(D1):D570-d8.

42. Steinegger M, Söding J. MMseqs2 enables sensitive protein sequence searching for the analysis of massive data sets. Nat Biotechnol. 2017;35(11):1026-8.

43. Jumper J, Evans R, Pritzel A, Green T, Figurnov M, Ronneberger O, et al. Highly accurate protein structure prediction with AlphaFold. Nature. 2021;596(7873):583-9.

44. Janson G, Zhang C, Prado MG, Paiardini A. PyMod 2.0: improvements in protein sequence-structure analysis and homology modeling within PyMOL. Bioinformatics. 2017;33(3):444-6.

45. Weigel LM, Brandt ME, Norgard MV. Analysis of the N-terminal region of the 47-kilodalton integral membrane lipoprotein of *Treponema pallidum*. Infect Immun. 1992;60(4):1568-76.

46. Murata T, Ohnishi M, Ara T, Kaneko J, Han CG, Li YF, et al. Complete nucleotide sequence of plasmid Rts1: implications for evolution of large plasmid genomes. J Bacteriol. 2002;184(12):3194-202.

47. Baker-Zander SA, Fohn MJ, Lukehart SA. Development of cellular immunity to individual soluble antigens of *Treponema pallidum* during experimental syphilis. J Immunol. 1988;141(12):4363-9.

48. Arora N, Schuenemann VJ, Jager G, Peltzer A, Seitz A, Herbig A, et al. Origin of modern syphilis and emergence of a pandemic *Treponema pallidum* cluster. Nat Microbiol. 2016;2:16245.

49. Edmondson DG, Hu B, Norris SJ. Long-Term In Vitro Culture of the Syphilis Spirochete *Treponema pallidum* subsp. *pallidum*. mBio. 2018;9(3).

50. Lukehart SA, Marra CM. Isolation and laboratory maintenance of *Treponema pallidum*. Curr Protoc Microbiol. 2007;Chapter 12:Unit 12A.1.

51. Giacani L, Hevner K, Centurion-Lara A. Gene organization and transcriptional analysis of the *tprJ*, *tprI*, *tprG* and *tprF* loci in the Nichols and Sea 81-4 *Treponema pallidum* isolates. J Bacteriol. 2005;187(17):6084-93.

52. Giacani L, Molini B, Godornes C, Barrett L, Van Voorhis WC, Centurion-Lara A, et al. Quantitative analysis of *tpr* gene expression in *Treponema pallidum* isolates: differences among isolates and correlation with T-cell responsiveness in experimental syphilis. Infect Immun. 2007;75(1):104-12.

53. Giacani L, Molini B, Godornes C, Barrett L, Van Voorhis W, Centurion-Lara A, et al. Quantitative analysis of tpr gene expression in *Treponema pallidum* isolates: Differences among isolates and correlation with T-cell responsiveness in experimental syphilis. Infect Immun. 2007;75(1):104-12.

54. Bolger AM, Lohse M, Usadel B. Trimmomatic: a flexible trimmer for Illumina sequence data. Bioinformatics. 2014;30(15):2114-20.

55. Langmead B, Salzberg SL. Fast gapped-read alignment with Bowtie 2. Nat Methods. 2012;9(4):357-9.

56. Kearse M, Moir R, Wilson A, Stones-Havas S, Cheung M, Sturrock S, et al. Geneious Basic: an integrated and extendable desktop software platform for the organization and analysis of sequence data. Bioinformatics. 2012;28(12):1647-9.

57. Lieberman NAP, Lin MJ, Xie H, Shrestha L, Nguyen T, Huang ML, et al. *Treponema pallidum* genome sequencing from six continents reveals variability in vaccine candidate genes and dominance of Nichols clade strains in Madagascar. PLoS Negl Trop Dis. 2021;15(12):e0010063.

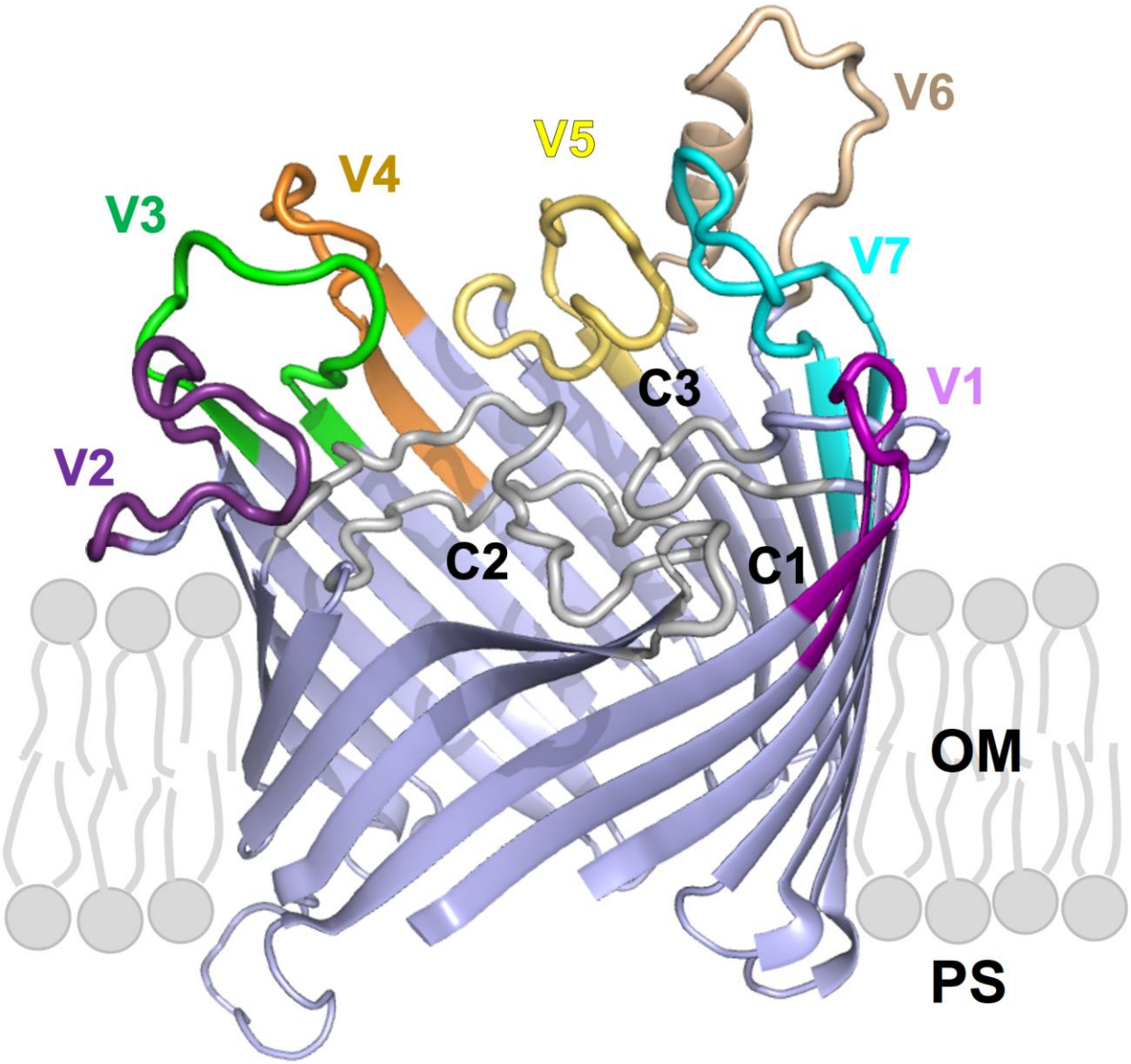
V6
V5
V4
V3
V7
V1
C3
V2
C2
C1
OM
PS

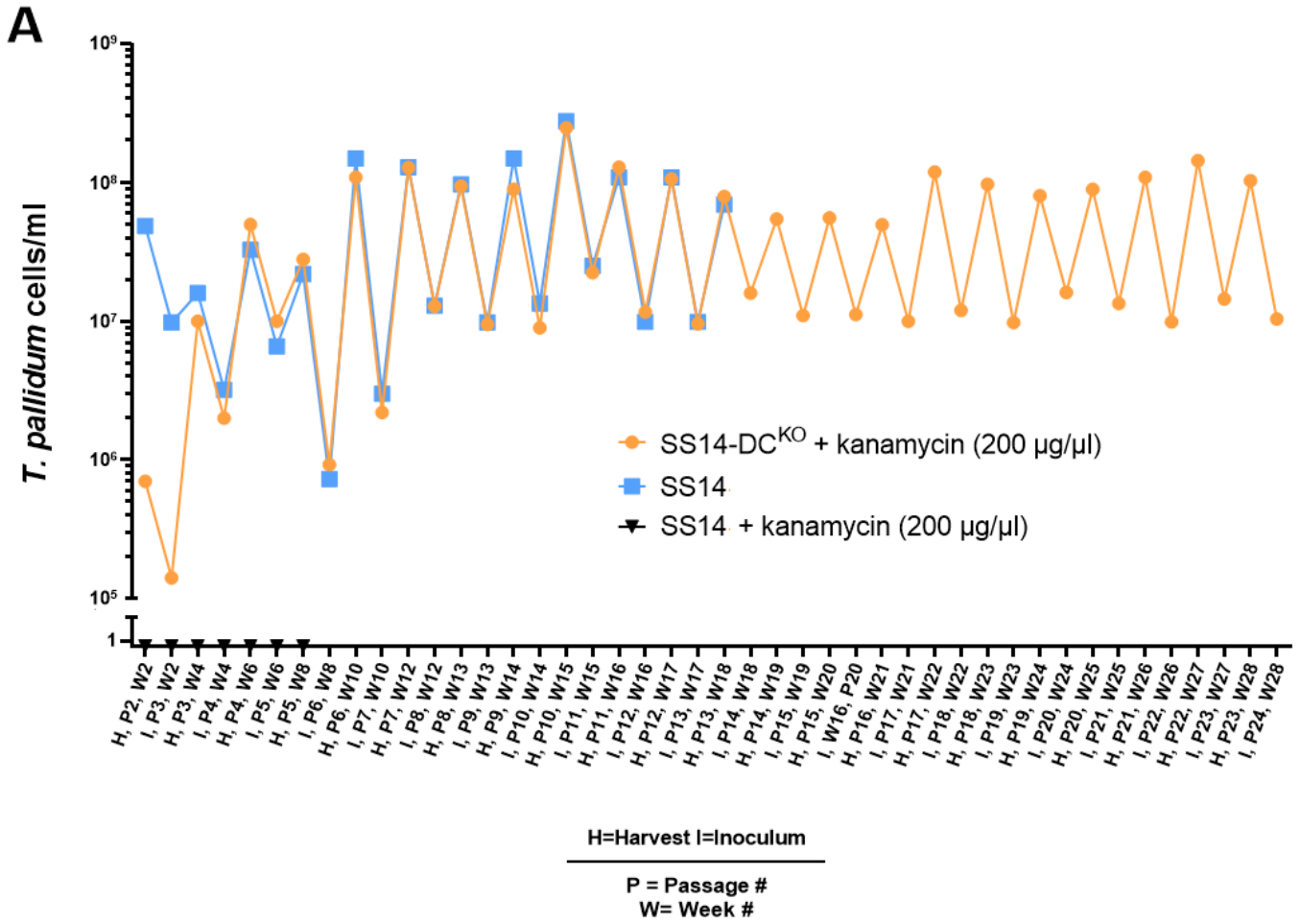
A
T. pallidum cells/ml
SS14-DC^KO + kanamycin (200 µg/µl)
SS14
SS14 + kanamycin (200 µg/µl)
H=Harvest I=Inoculum
P = Passage #
W= Week #

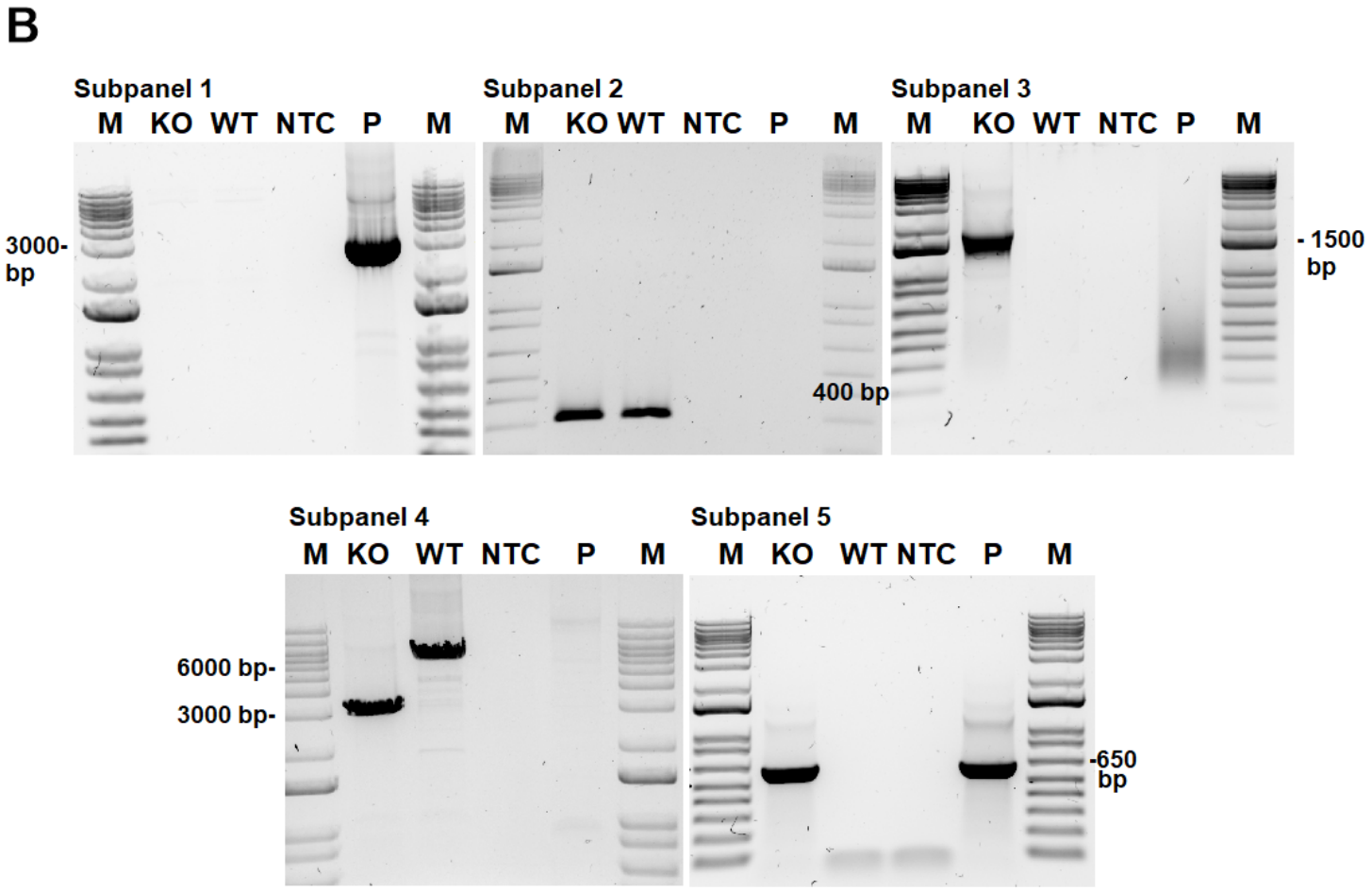
B
Subpanel 1
M KO WT NTC P M
3000-bp
Subpanel 2
M KO WT NTC P M
400 bp
Subpanel 3
M KO WT NTC P M
1500 bp
Subpanel 4
M KO WT NTC P M
6000 bp-
3000 bp-
Subpanel 5
M KO WT NTC P M
650 bp

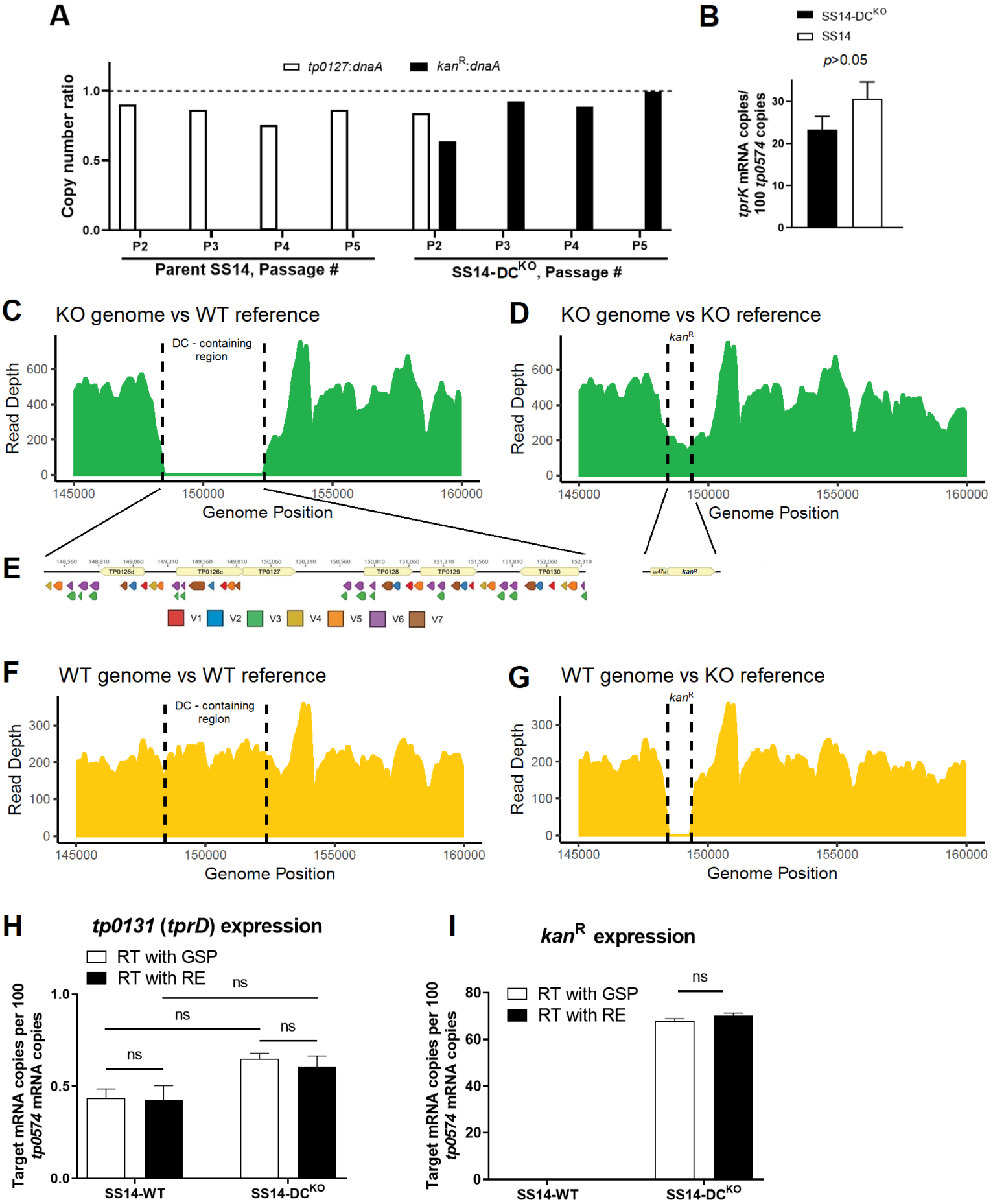
A
tp0127:dnaA
kanR:dnaA
Copy number ratio
1.0
0.5
0.0
P2
P3
P4
P5
Parent SS14, Passage #
SS14-DCKO, Passage #
B
SS14-DCKO
SS14
p>0.05
tprK mRNA copies/ 100 tp0574 copies
30
20
10
0
C
KO genome vs WT reference
DC - containing region
Read Depth
600
400
200
0
145000
150000
155000
160000
Genome Position
D
KO genome vs KO reference
kanR
Read Depth
600
400
200
0
145000
150000
155000
160000
Genome Position
E
TP0126d
TP0126c
TP0127
TP0128
TP0129
TP0130
tp47p
kanR
V1
V2
V3
V4
V5
V6
V7
F
WT genome vs WT reference
DC - containing region
Read Depth
300
200
100
0
145000
150000
155000
160000
Genome Position
G
WT genome vs KO reference
kanR
Read Depth
300
200
100
0
145000
150000
155000
160000
Genome Position
H
tp0131 (tprD) expression
RT with GSP
RT with RE
ns
ns
ns
ns
Target mRNA copies per 100 tp0574 mRNA copies
1.0
0.5
0.0
SS14-WT
SS14-DCKO
I
kanR expression
RT with GSP
RT with RE
ns
Target mRNA copies per 100 tp0574 mRNA copies
80
60
40
20
0
SS14-WT
SS14-DCKO

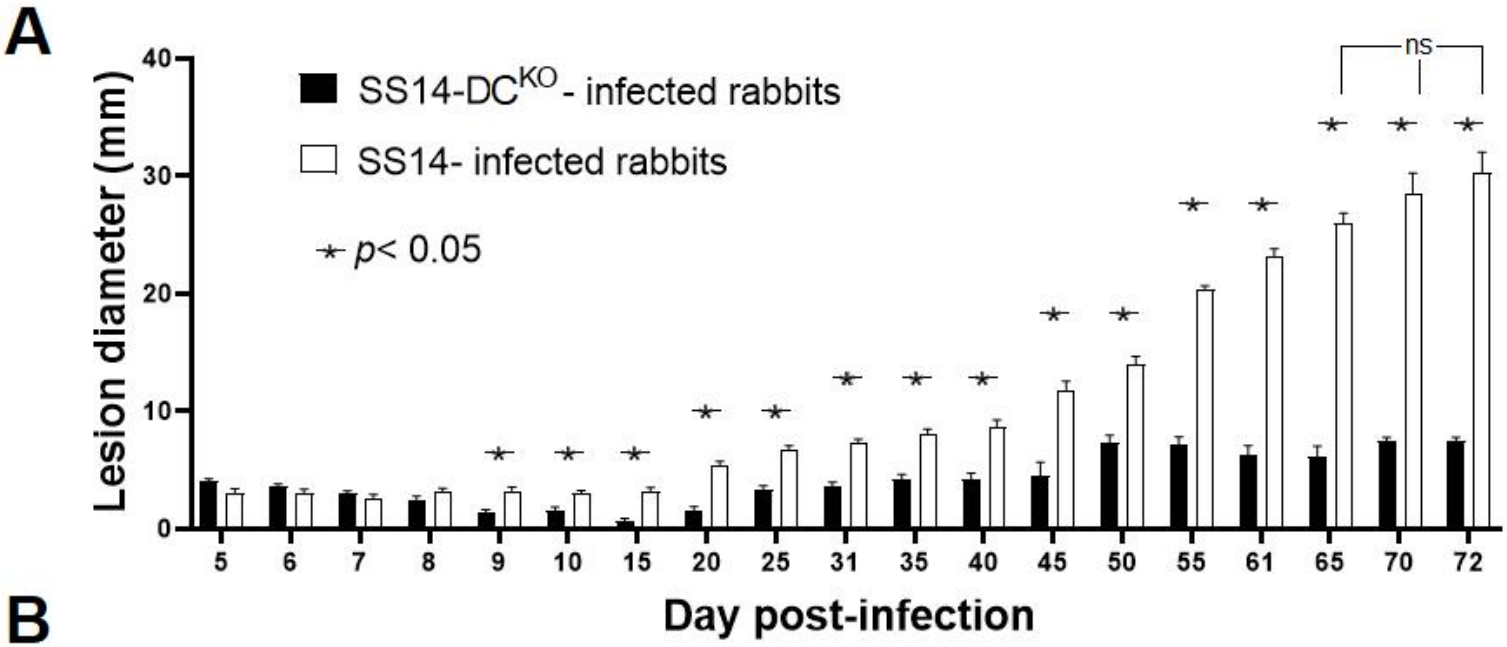

B

SS14-DC^{KO} –infected rabbits (day 72 PI)

SS14–infected rabbits (day 72 PI)

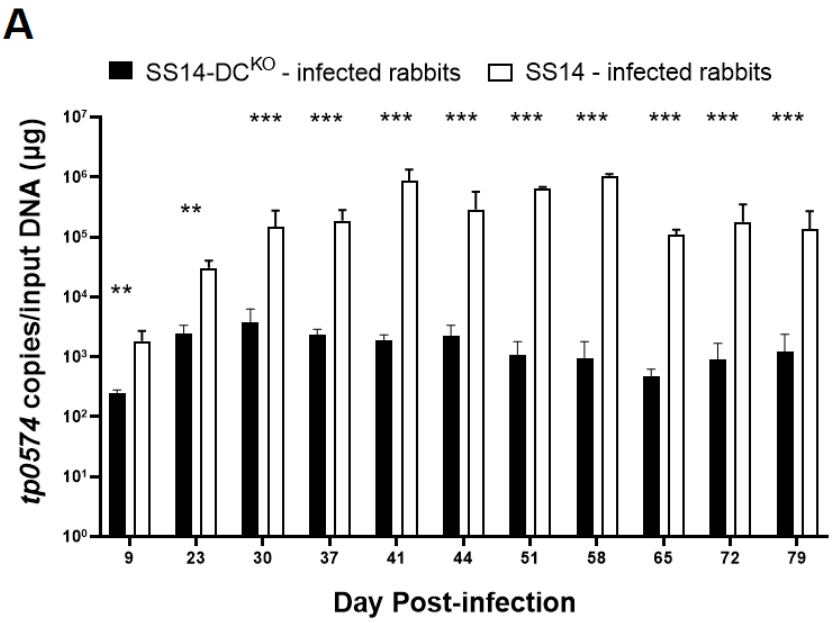
A
SS14-DC^KO - infected rabbits
SS14 - infected rabbits
tp0574 copies/input DNA (µg)
Day Post-infection

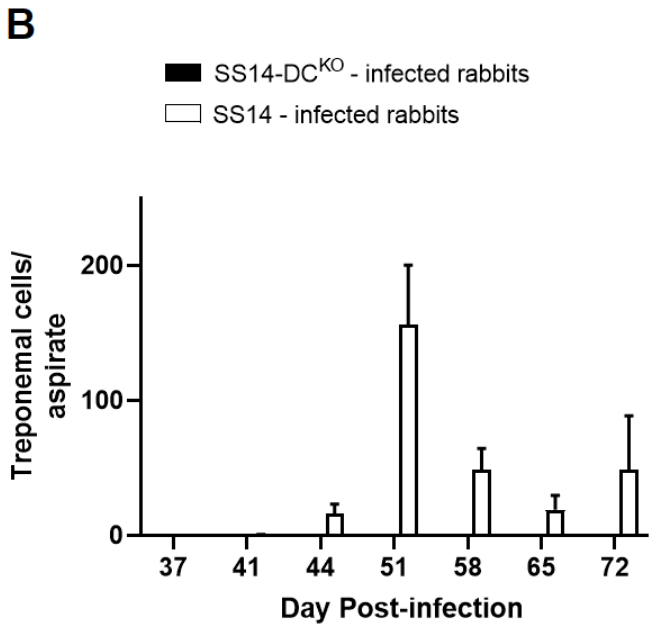
B
SS14-DC^KO - infected rabbits
SS14 - infected rabbits
Treponemal cells/ aspirate
Day Post-infection

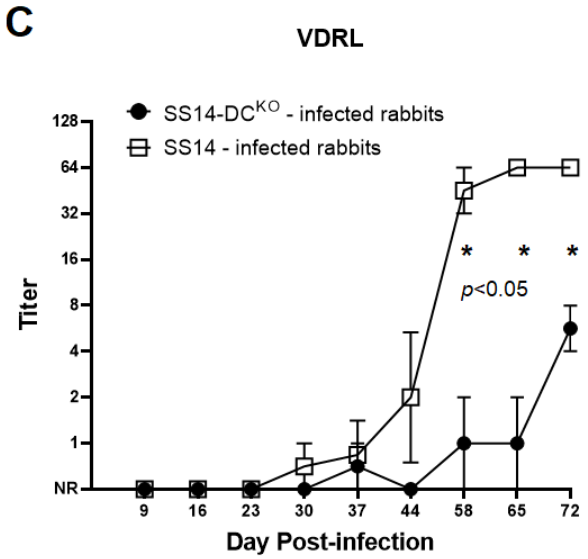
C
VDRL
SS14-DC^KO - infected rabbits
SS14 - infected rabbits
Titer
p<0.05
Day Post-infection

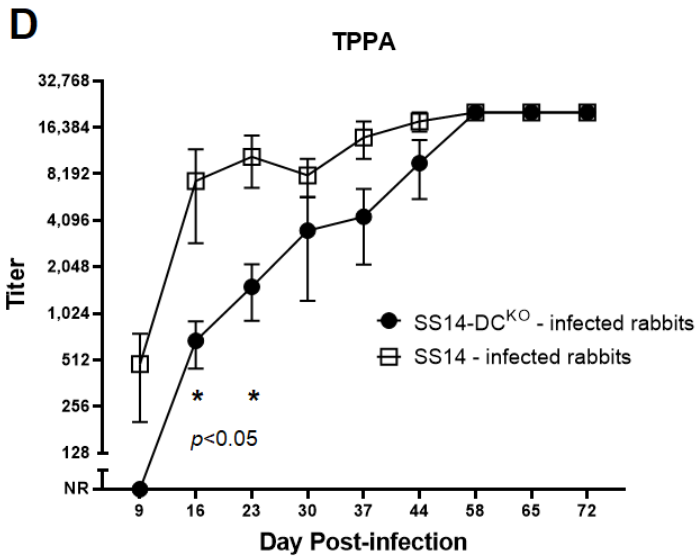
D
TPPA
Titer
SS14-DC^KO - infected rabbits
SS14 - infected rabbits
p<0.05
Day Post-infection

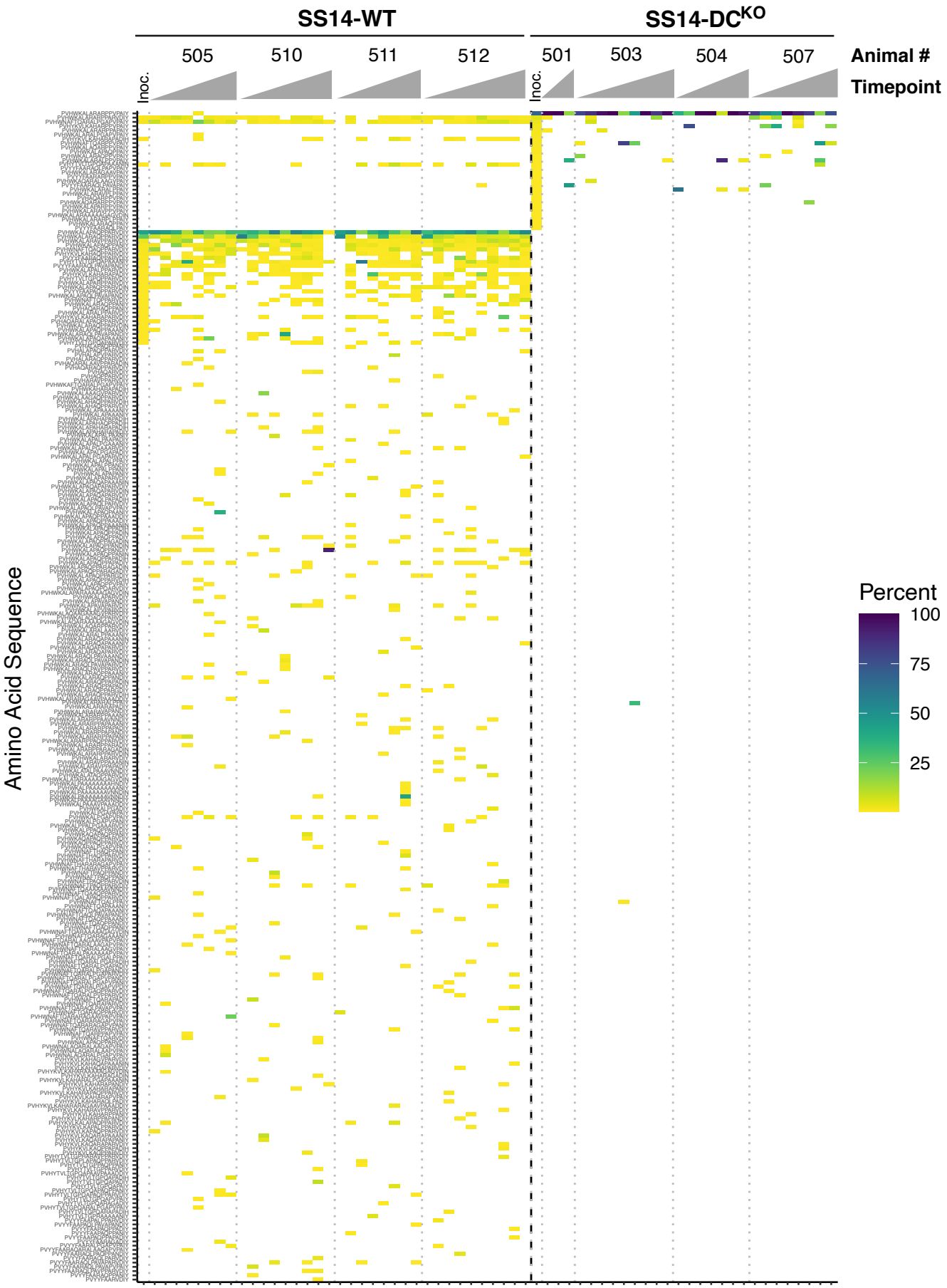
SS14-WT
SS14-DC^KO
505
510
511
512
501
503
504
507
Animal #
Timepoint
Inoc.
Inoc.
Amino Acid Sequence
Percent
100
75
50
25

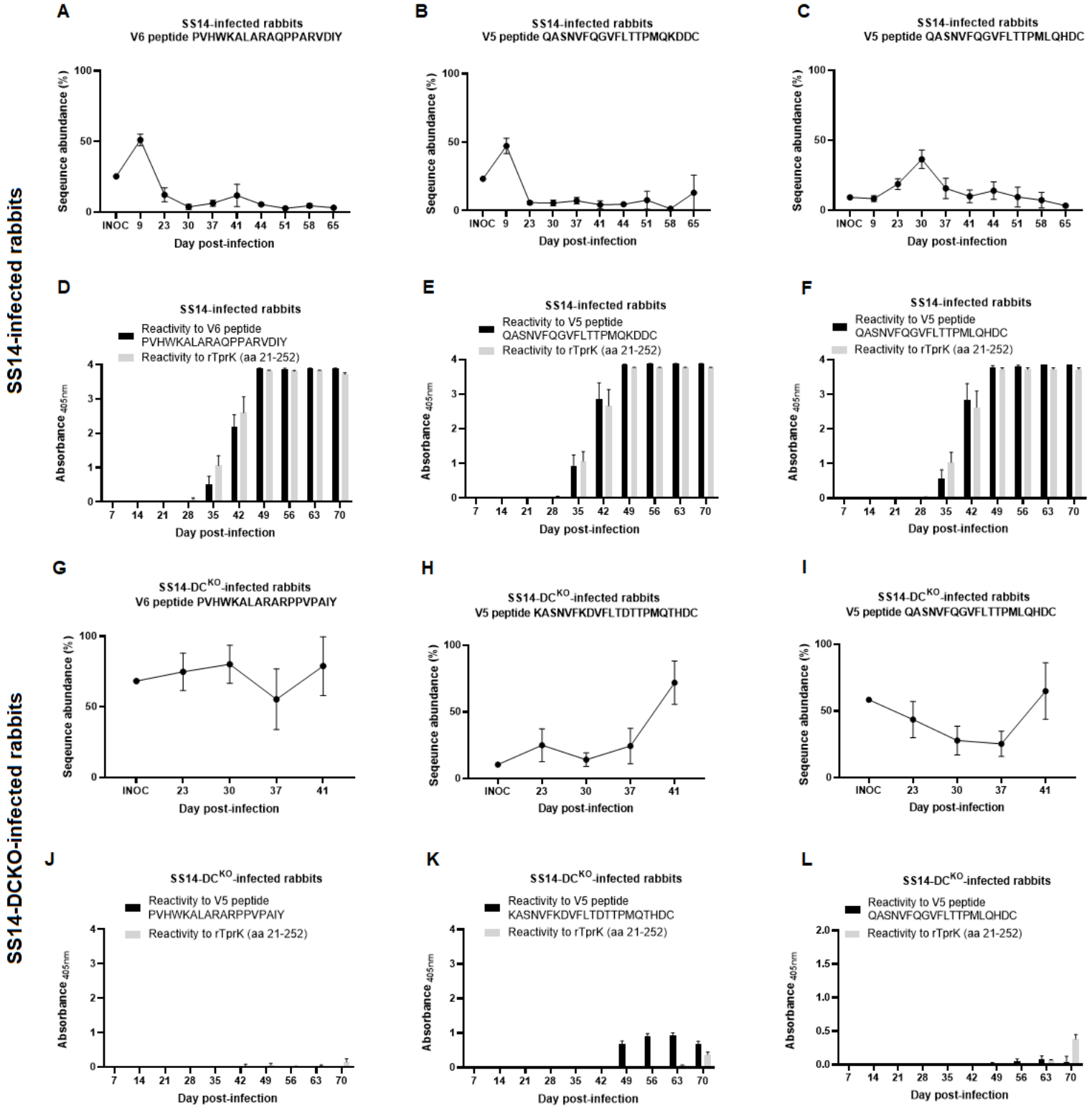
SS14-infected rabbits
SS14-DCKO-infected rabbits
A
SS14-infected rabbits
V6 peptide PVHWKALARAQPPARVDIY
Seqeunce abundance (%)
Day post-infection
B
SS14-infected rabbits
V5 peptide QASNVFQGVFLTTPMQKDDC
C
SS14-infected rabbits
V5 peptide QASNVFQGVFLTTPMLQHDC
D
SS14-infected rabbits
Reactivity to V6 peptide PVHWKALARAQPPARVDIY
Reactivity to rTprK (aa 21-252)
Absorbance 405nm
E
Reactivity to V5 peptide QASNVFQGVFLTTPMQKDDC
F
Reactivity to V5 peptide QASNVFQGVFLTTPMLQHDC
G
SS14-DC^KO-infected rabbits
V6 peptide PVHWKALARARPPVPAIY
H
V5 peptide KASNVFKDVFLTDTTPMQTHDC
I
V5 peptide QASNVFQGVFLTTPMLQHDC
J
Reactivity to V5 peptide PVHWKALARARPPVPAIY
K
Reactivity to V5 peptide KASNVFKDVFLTDTTPMQTHDC
L
Reactivity to V5 peptide QASNVFQGVFLTTPMLQHDC